Novel imidazo[4,5-*b*]pyridine derived acrylonitriles: A combined experimental and computational study of their antioxidative potential

Ida Boček,[1] Kristina Starčević,[2] Ivana Novak Jovanović,[3] Robert Vianello,[4]* Marijana Hranjec[1]*

[1]*Department of Organic Chemistry, Faculty of Chemical Engineering and Technology, University of Zagreb, Marulićev trg 19, 10000 Zagreb, Croatia.*

[2]*Department of Animal Husbandry, Faculty of Veterinary Medicine, University of Zagreb, Heinzelova 55, 10000 Zagreb, Croatia.*

[3]*Institute for Medical Research and Occupational Health, Ksaverska cesta 2, 10000 Zagreb, Croatia.*

[4]*Laboratory for the computational design and synthesis of functional materials, Division of Organic Chemistry and Biochemistry, Ruđer Bošković Institute, Bijenička 54, 10000 Zagreb, Croatia.*

**Corresponding authors: robert.vianello@irb.hr (R.V.); mhranjec@fkit.hr (M.H.)*

ABSTRACT: We describe the synthesis of novel unsubstituted and *N*-substituted imidazo[4,5-*b*]pyridine derived acrylonitriles, which were prepared by classical and microwave assisted organic synthesis. Their antioxidative potential was studied using spectroscopic DPPH and ABTS assays, FRAP method and electrochemical oxidation potential measurements. Targeted acrylonitriles were designed in order to study the influence of the methoxy, *N,N*-dimethylamino and *N,N*-diethylamino substituents on the antioxidative activity as well as the type of the substituent placed on the N-atom of the imidazo[4,5-*b*]pyridine nuclei. The most active derivatives with significantly improved activity relative to the standard BHT, were systems substituted with the *N,N*-$(CH_3)_2$ group **29** and the *N,N*-$(CH_2CH_3)_2$ group at the *para* position of the phenyl ring **24**, **30**, **32** and **34**. Computational analysis revealed that investigated antioxidative features are predominantly relying on the hydrogen atom transfer properties and can be efficiently enhanced through either the *N*-alkylation of the imidazole nitrogen or by introducing electron-donating substituents on the distant phenyl unit, where *N*,*N*-dialkylamines prevail over methoxy groups. Absorption spectra of chosen compounds were recorded in several organic solvents to further reveal the impact of the substituent effects and solvent polarity on spectroscopic features.

KEYWORDS: acrylonitriles; antioxidative potential; DFT calculations; electrochemical oxidation potential; imidazo[4,5-*b*]pyridines; solvent effects

1. INTRODUCTION

One of the most privileged structural motifs in organic and medicinal chemistry is nitrogen containing heterocycles that are indispensable structural fragments in designing novel biologically active molecules in pharmaceutical industry [1]. Some of nitrogen heterocycles like pyridines, benzimidazoles and/or imidazo[4,5-*b*]pyridines have a great significance in medicinal chemistry due to their structural similarity with naturally occurring purines, which allowed medicinal chemists the optimization of these skeletons towards more efficient and selective molecules that could be of a particular interest in drug discovery [2,3]. Among a wide range of different biological features displayed by versatile imidazo-pyridine derivatives, the most promising are antitumor, antimicrobial and antiviral activities which offered suchlike derivatives to have an important role in the prevention of numerous diseases [4].

On the other hand, the antioxidative potential of imidazo[4,5-*b*]pyridine derivatives is still unexplored with numerous possibilities for the imidazo[4,5-*b*]pyridine functionalization to explore their antioxidative potential. A group of authors described the synthesis and antioxidative potential of several 6-chloro-2-aryl-1*H*-imidazo[4,5-*b*]pyridine derivatives with different type and number of substituent placed at the phenyl ring [5]. Taking into account the structural similarity of benzimidazole and imidazo[4,5-*b*]pyridine nuclei and the facts that recently we have published several papers confirming a promising antioxidative potential of versatile benzimidazole derivatives [6–8] (Fig. 1), and insufficiently explored antioxidative potential of heteroaromatic acrylonitrile derivatives, we have designed and prepared novel imidazo[4,5-*b*]pyridine derived acrylonitriles as potential antioxidative agents.

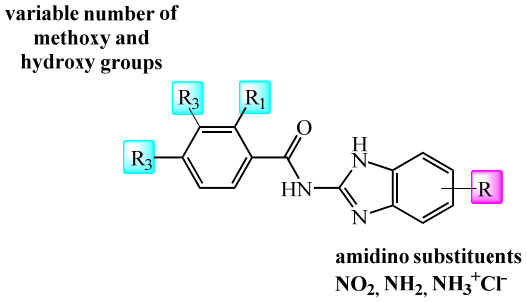

Figure 1. Recently published benzimidazole-2-carboxamides with antioxidative potential.

There still is a great interest in designing and developing novel, more efficient antioxidants despite the fact that there are numerous well known natural and synthetic molecules possessing notable antioxidative potential [9,10]. Antioxidants are important to avert or remove oxidative stress related diseases caused by ROS (reactive oxygen species), usually by mollifying free radicals, thereby playing a crucial role in conserving finest cellular functions [11,12]. It is well known that there is an implication of ROS in the cell signalling pathway of many chronic diseases, like diabetes mellitus, myocardial infarction, atherosclerosis, arthritis, inflammation or neurodegenerative diseases as well as a breakdown of the peptide chains caused by oxidation or lipid peroxidation [13,14]. Taking into account that we have recently

confirmed that the number of methoxy and/or hydroxyl groups as well as the type of nitro, amino and amidino substituent have a strong impact on the antioxidative potential of some benzazole and benzamide derivatives, we have designed novel acrylonitrile derived imidazo[4,5-*b*]pyridine analogues substituted with a variable number of methoxy groups, and *N,N*-dimethylamino and *N,N*-diethylamino group placed at the phenyl nuclei. Additionally, our attention was to study the influence of the substituent placed at the N atom of imidazo[4,5-*b*]pyridine fragment on the antioxidative potential examined by several methods, as well as to use computational analysis to interpret the observed trends in measured antioxidative potentials.

2. MATERIALS AND METHODS

2.1. CHEMISTRY

2.1.1. General Methods

All chemicals and solvents were purchased from commercial suppliers Aldrich, Acros and Fluka. Melting points were recorded on SMP11 Bibby apparatus and were not corrected. All NMR spectra were measured in DMSO-d_6 solutions using TMS as an internal standard. The ^{1}H and ^{13}C NMR spectra were recorded on a Varian Bruker Avance III HD 400 MHz/54 mm Ascend, Bruker AV300 or Bruker AV600 spectrophotometer at 300, 400, 600, 150, 100 and 75 MHz respectively. Chemical shifts are reported in ppm (δ) relative to TMS. All compounds were routinely checked by thin layer chromatography with Merck silica gel 60F-254 plates and the spots were detected under UV light (254 nm). Column chromatography was performed using silica gel (0.063–0.2 mm) Fluka; glass column was slurry-packed under gravity. Microwave-assisted synthesis was performed in a Milestone start S microwave oven using quartz cuvettes under the pressure of 40 bar or using pyrex cuvettes under the pressure of 1 bar.

2.1.2. General method for preparation of compounds 2–4

Compounds **2–4** were prepared using microwave irradiation for 1 h at 170 °C with power 800 W and 40 bar pressure, from 1 in acetonitrile (10 mL) with excess of added corresponding amine. After cooling, resulting product was purified by column chromatography on SiO_2 using dichlormethane as eluent.

3-nitro-N-phenylpyridin-2-amine ***2***

2 was prepared using above described method from 1 (0.50 g, 3.15 mmol) and aniline (1.47 mL, 15.75 mmol) after 1 h of irradiation to yield 0.57 g (82%) of red crystals; m.p. 77-78 °C; ^{1}H NMR (300 MHz, DMSO) (δ/ppm): 9.96 (s, 1H, NH), 8.58 – 8.48 (m, 2H, H_{arom}), 7.65 (d, J = 7.7 Hz, 2H, H_{arom}), 7.37 (t, J = 7.9 Hz, 2H, H_{arom}), 7.14 (t, J = 7.4 Hz, 1H H_{arom}), 6.99 (dd, J_1 = 8.3 Hz, J_2 = 4.6 Hz, 1H, H_{arom}); APT ^{13}C NMR (75 MHz, DMSO) (δ/ppm): 155.52, 149.97, 138.83, 136.07, 129.28, 129.08 (2C), 124.59, 123.21 (2C), 114.96. Anal. Calcd. for $C_{11}H_9N_3O_2$: C, 61.39; H, 4.22; N, 19.53; O, 14.87. Found: 61.01; H, 4.15; N, 19.74; O, 14.98%.

*N-isobutyl-3-nitropyridin-2-amine **3***

3 was prepared using above described method from 1 (0.50 g, 3.15 mmol) and isobutylamine (1.57 mL, 15.75 mmol) after 1 h of irradiation to yield 0.60 g (97%) of yellow oil; ^{1}H NMR (600 MHz, DMSO) (δ/ppm): 8.48 (dd, J_1 = 4.4 Hz, J_2 = 1.8 Hz, 1H, H_{arom}), 8.47 (bs, 1H, NH), 8.41 (dd, J_1 = 8.4 Hz, J_2 = 1.7 Hz, 1H, Harom), 6.75 (dd, J_1 = 8.3 Hz, J_2 = 4.4 Hz, 1H, H_{arom}), 3.42 (t, J = 6.5 Hz, 2H, CH_2), 1.97 (m, 1H, CH), 0.97 (d, J = 6.7 Hz, 6H, CH_3); ^{13}C NMR (75 MHz, DMSO) (δ/ppm): 156.60, 152.67, 135.78, 127.71, 112.21, 48.30, 28.02, 20.50 (2C). Anal. Calcd. for $C_9H_{13}N_3O_2$: C, 55.37; H, 6.71; N, 21.52; O, 16.39. Found: C, 55.20; H, 6.80; N, 21.42; O, 16.20%.

*N-methyl-3-nitropyridin-2-amine **4***

4 was prepared using above described method from 1 (0.50 g, 3.15 mmol) and methylamine (1.96 mL, 15.75 mmol) after 1 h of irradiation to yield 0.42 g (88%) of yellow crystals; m.p. 70-71 °C; ^{1}H NMR (600 MHz, DMSO) (δ/ppm): 8.50 (dd, J_1= 4.4 Hz, J_2 = 1.7 Hz, 1H, H_{arom}), 8.47 (s, 1H, NH), 8.41 (dd, J_1= 8.3, J_2 = 1.7 Hz, 1H, H_{arom}), 6.75 (dd, J_1 = 8.3 Hz, J_2 = 4.4 Hz, 1H, H_{arom}), 3.04 (d, J = 4.7 Hz, 6H, CH_3); APT ^{13}C NMR (151 MHz, DMSO) (δ/ppm): 156.05, 152.41, 135.09, 127.58, 111.48, 28.23. Anal. Calcd. for $C_6H_7N_3O_2$:, C, 47.06; H, 4.61; N, 27.44; O, 20.89. Found: C, 46.96; H, 4.80; N, 27.21; O, 21.01%.

*N^2-phenylpyridine-2,3-diamine **5***

5 was prepared using microwave irradiation for 19 minutes at 110 °C with power of 300 W, from 0.50 g (2.32 mmol) of 3-nitro-N-phenylpyridin-2-amine 2 and $SnCl_2 \times 2H_2O$ 2.62 g (11.61 mmol) in methanol (10 mL). After cooling, the reaction mixture was evaporated under vacuum and dissolved in water (10 mL). The resulting solution was treated with 20% NaOH to pH = 14. The resulting precipitate was filtered off, washed with hot ethanol and filtered. The filtrate was evaporated at a reduced pressure, a small amount of water was added and the product was filtered to obtain white crystals 0.24 g (57 %); m.p. 151-153 °C; ^{1}H NMR (300 MHz, DMSO) (δ/ppm): 7.70 (s, 1H, NH), 7.63 (dd, J_1 = 8.7 Hz, J_2 = 1.0 Hz, 2H, H_{arom}), 7.50 (dd, J_1 = 4.8 Hz, J_2 = 1.6 Hz, 1H, H_{arom}), 7.26 – 7.19 (m, 2H, H_{arom}), 6.90 (dd, J_1= 7.6 Hz, J_2 = 1.7 Hz, 1H, H_{arom}), 6.84 (t, J = 7.3 Hz, 1H H_{arom}), 6.62 (dd, J_1 = 7.6 Hz, J_2 = 4.8 Hz, 1H, H_{arom}), 5.06 (s, 2H, NH_2); APT ^{13}C NMR (151 MHz, DMSO) (δ/ppm): 143.62, 142.23, 134.34, 131.85, 128.27 (2C), 119.80, 119.60, 118.01 (2C), 115.70. Anal. Calcd. for $C_{11}H_{11}N_3$: C, 71.33; H, 5.99; N, 22.69. Found: C, 71.05; H, 6.17; N, 22.87%.

2.1.3. General method for preparation of compounds 6–7

Compounds **6–7** were prepared using microwave irradiation in pyrex microwave cuvettes using 5 w% of Pd/C and ammonium formate as source of hydrogen. Reaction mixture was irradiated for few minutes at 60 °C with power 300 W until TLC indicated end of reaction. After cooling, the reaction mixture was filtered over a celite bed and filtrate was evaporated at a reduced pressure. Compounds were used in the next step without further purification.

N^2-isobutylpyridine-2,3-diamine ***6***

6 was prepared using above described method from **4** (0.50 g, 2.56 mmol), ammonium formate (0.65 g, 10.22 mmol) and 0.025 g of Pd/C after 6 min of irradiation to obtain dark oil 0.36 g (85%); ^{1}H NMR (300 MHz, DMSO) (δ/ppm): 7.33 (dd, J_1 = 5.0 Hz, J_2 = 1.6 Hz, 1H H_{arom}), 6.64 (dd, J_1 = 7.4 Hz, J_2 = 1.6 Hz, 1H H_{arom}), 6.30 (dd, J_1 = 7.4 Hz, J_2 = 5.0 Hz, 1H, H_{arom}), 5.5 (bs, 1H, NH), 4.67 (bs, 2H, NH_2), 3.12 (t, J = 6.2 Hz, 2H, CH_2), 1.87 (m, 1H, CH), 0.90 (d, J = 6.7 Hz, 6H, CH_3); APT ^{13}C NMR (151 MHz, DMSO) (δ/ppm): 147.96, 134.82, 129.93, 117.24, 111.82, 48.70, 27.49, 20.46 (2C). Anal. Calcd. for $C_9H_{15}N_3$: C, 65.42; H, 9.15; N, 25.43. Found: C, 65.19; H, 9.23; N, 25.15%.

N^2-methylpyridine-2,3-diamine ***7***

7 was prepared using above described method from **5** (0.50 g, 3.26 mmol) ammonium formate (0.82 g, 12.90 mmol) and 0.025 g of Pd/C after 6 min of irradiation to yield 0.21 g (52%) of dark purple oil.^{1}H NMR (600 MHz, DMSO) (δ/ppm): 7.38 (dd, J_1 = 5.0 Hz, J_2 = 1.5 Hz, 1H, H_{arom}), 6.65 (dd, J_1 = 7.4 Hz, J_2 = 1.5 Hz, 1H, H_{arom}), 6.32 (dd, J_1 = 7.3 Hz, J_2 = 5.0 Hz, 1H, H_{arom}), 5.54 (d, J = 4.2 Hz, 1H, NH), 4.59 (s, 2H, NH_2), 2.81 (d, 3H, J = 4.7 Hz, 3H, CH_3); APT ^{13}C NMR (151 MHz, DMSO) (δ/ppm): 148.58, 134.97, 130.25, 117.04, 111.99, 28.10. Anal. Calcd. for $C_6H_9N_3$: C, 58.51; H, 7.37; N, 34.12. Found: C, 58.65; H, 7.20; N, 34.67%.

2.1.4. General method for preparation of compounds 9–12

Compounds **9–12** were prepared by heating a mixture of corresponding 2,3-diaminopyridines and ethyl-cyanoacetate in oil bath at 190 °C. After cooling, reaction mixture was treated with ether and resulting product was filtered off and, if necessary, recrystallized.

2-(3-phenyl-3H-imidazo[4,5-b]pyridin-2-yl)acetonitrile ***9***

9 was prepared using above described method from **5** (0.50 g, 2.70 mmol) and ethyl-cyanoacetate (0.43 mL, 4.05 mmol) after 45 min of heating to yield after recrystalization from 20% ethanol 0.27 g (42%) of white crystals; m.p. 183-185 °C; ^{1}H NMR (400 MHz, DMSO) (δ/ppm): 8.32 (dd, J_1 = 4.8 Hz, J_2 = 1.4 Hz, 1H, H_{arom}), 8.20 (dd, J_1 = 8.0 Hz, J_2 = 1.4 Hz, 1H, H_{arom}), 7.68 – 7.57 (m, 5H, H_{arom}), 7.38 (dd, J_1 = 8.0 Hz, J_2 = 4.8 Hz, 1H, H_{arom}), 4.44 (s, 2H, CH_2); APT ^{13}C NMR (101 MHz, DMSO) (δ/ppm): 149.15, 147.34, 144.83, 134.23, 133.87, 130.13 (2C), 129.70, 128.06 (2C), 127.64, 119.61, 116.18, 19.35. Anal. Calcd. for $C_{14}H_{10}N_4$: C, 71.78; H, 4.30; N, 23.92. Found: C, 71.63; H, 4.35; N, 23.79%.

2-(3-isobutyl-3H-imidazo[4,5-b]pyridin-2-yl)acetonitrile ***10***

10 was prepared from **6** (0.71 g, 4.30 mmol) and ethyl-cyanoacetate (0.69 mL, 6.45 mmol) after 1 h of irradiation to yield 0.42 g (46%) of dark green crystals; m.p. 115-116 °C; ^{1}H NMR (400 MHz, DMSO) (δ/ppm): 8.36 (dd, J_1 = 4.8 Hz, J_2 = 1.4 Hz, 1H, H_{arom}), 8.08 (dd, J_1 = 8.0 Hz, J_2 = 1.4 Hz, 1H, H_{arom}), 7.30 (dd, J_1 = 8.0 Hz, J_2 = 4.8 Hz, 1H, Harom), 4.61 (bs, 2H, CH_2), 4.08 (d, J = 7.7 Hz, 2H, NH_2), 2.31-2.18 (m, 1H, CH), 0.86 (d, J = 6.7 Hz, 6H, CH_3); APT ^{13}C NMR (101 MHz, DMSO) (δ/ppm): 148.66, 147.66, 144.16, 134.19, 127.24, 118.86,

116.57, 49.48, 28.57, 20.13, 18.55 (2C). Anal. Calcd. For: $C_{12}H_{14}N_4$: C, 67.27; H, 6.59; N, 26.15. Found: C, 67.01; H, 6.50; N, 26.21%.

*2-(3-methyl-3H-imidazo[4,5-b]pyridin-2-yl)acetonitrile **11***

11 was prepared from **7** (0.58 g, 4.71mmol) and ethyl-cyanoacetate (0.75 mL, 7.07 mmol) after 45 min of heating to yield 0.42 g (46%) of brown powder; m.p. 146 °C; ^{1}H NMR (400 MHz, DMSO) (δ/ppm): 8.34 (dd, J_1 = 4.7 Hz, J_2 = 1.1 Hz, 1H, H_{arom}), 8.05 (dd, J_1 = 7,9 Hz, J_2 = 1.2 Hz, 1H, H_{arom}), 7.28 (dd, J_1 = 8.0 Hz, J_2 = 4.7 Hz, H_{arom}). 4.58 (s, 2H, CH_2), 3.75 (s, 3H, CH_3); APT ^{13}C NMR (151 MHz, DMSO) (δ/ppm): 148.10, 147.50, 143.53, 133.81, 126.66, 118.25, 115.84, 28.23, 17.95. Anal. Calcd. For: $C_9H_8N_4$: C, 62.78; H, 4.68; N, 32.54. Found: C, 62.57; H, 4.69; N, 32.23%.

*2-(3H-imidazo[4,5-b]pyridin-2-yl)acetonitrile **12***

12 was prepared from 2,3-diaminopyridine **8** (1.00 g, 9.16 mmol) and ethyl-cyanoacetate (1.5 mL, 13.74 mmol) after 30 min of heating to yield 1.2 g (83%) of brown powder. mp 268–271 °C; ^{1}H NMR (300 MHz, DMSO) (δ/ppm): 13.06 (bs, 1H, NH), 8.34 (s, 1H, H_{arom}), 8.00 (s, 1H, H_{arom}), 7.25 (dd, J_1 = 8.0 Hz, J_2 = 4.8 Hz, 1H, H_{arom}), 4.42 (s, 2H, CH_2); APT ^{13}C NMR (75 MHz, DMSO) (δ/ppm): 143.73, 118.00 (2C), 116.17, 18.73. Anal. Calcd. For: $C_8H_6N_4$: C, 60.75; H, 3.82; N, 35.42. Found: C, 60.60; H, 3.79; N, 35.55%.

2.1.5. General method for preparation of compounds 19–32

Solution of equimolar amounts of 2-cyanomethylimidazo[4,5-*b*]pyridines **9–12**, corresponding aromatic aldehydes **13**–**18** and few drops of piperidine in absolute ethanol, were refluxed for 2 hours. The cooled reaction mixture was filtered and, if necessary, product was purified by column chromatography on SiO_2 using dichloromethane/methanol as eluent.

*(E)-3-phenyl-2-(3-phenyl-3H-imidazo[4,5-b]pyridin-2-yl)acrylonitrile **19***

19 was prepared from **9** (0.07 g, 0.30 mmol) and 13 (0.05 g, 0.30 mmol) in absolute ethanol (2 mL) after refluxing for 1.5 hours to yield 0.03 g (30%) light yellow powder; m.p. 97-101 °C; ^{1}H NMR (600 MHz, DMSO) (δ/ppm): 8.39 (dd, J_1 = 4.7 Hz, J_2 = 1.4 Hz,1H, H_{arom}), 8.27 (dd, J_1 = 8.1 Hz, J_2 = 1.4 Hz, 1H, H_{arom}), 7.94 (s, 1H, CH), 7.82 – 7.80 (d, J = 7,3 Hz, 2H, H_{arom}), 7.66 – 7.62 (m, 4H, H_{arom}), 7.61 – 7.58 (m, 1H, H_{arom}), 7.57 – 7.52 (m, 3H, H_{arom}), 7.45 (dd, J_1 = 8.1 Hz, J_2 = 4,7 Hz, 1H, H_{arom}); APT ^{13}C NMR (151 MHz, DMSO) (δ/ppm): 151.16, 148.90, 147.66, 145.34, 134.15, 134.04, 132.23, 132.22, 132.21, 129.64, 129.61, 129.38, 129.24, 129.10, 128.82, 128.11, 127.60, 126.64, 119.83, 115.26 (2C), 100.59. MS (ESI): m/z= 323.03 ($[M+1]^+$). Anal. Calcd. For: $C_{21}H_{14}N_4$: C, 78.24; H, 4.38; N, 17.38. Found: C, 78.02; H, 4.44; N, 17.38%.

*(E)-3-(2-methoxyphenyl)-2-(3-phenyl-3H-imidazo[4,5-b]pyridin-2-yl)acrylonitrile **20***

20 was prepared from **9** (0.07 g, 0.30 mmol) and 14 (0.04 g, 0.30 mmol) in absolute ethanol (2 mL) after refluxing for 1.5 hours to yield 0.05 g (47%) light yellow powder; m.p. >300 °C; ^{1}H NMR (400 MHz, DMSO) (δ/ppm): 8.37 (dd, J_1 = 4.7 Hz, J_2 = 1.4 Hz, 1H, H_{arom}), 8.27 (dd, J_1 = 8.0 Hz, J_2 = 1.4 Hz, 1H, H_{arom}), 8.05 (dd, J_1 = 7.4 Hz, J_2 = 1,6 Hz,1H, H_{arom}), 8.04 (s, 1H, CH) 7.67 – 7.61 (m, 5H, H_{arom}), 7.57 – 7.52 (m, 1H, H_{arom}), 7.44 (dd,

J_1 = 8.0 Hz, J_2 = 4.7 Hz, 1H, H_{arom}), 7.11 (m, 2H, H_{arom}), 3.75 (s, 3H. OCH_3); APT ^{13}C NMR (101 MHz, DMSO) (δ/ppm): 158.61, 149.65, 148.34, 145.74, 145.29, 134.89 (2C), 134.57, 130.26 (2C), 129.84, 128.68 (2C), 128.18, 128.02, 121.28, 121.14, 120.23, 116.10, 112.40, 101.26, 56.22. MS (ESI): m/z= 352.80 ($[M+1]^+$). Anal. Calcd. For: $C_{22}H_{16}N_4O$: C, 74.98; H, 4.58; N, 15.90; O, 4.54. Found: C, 75.05; H, 4.65; N, 15.80; O, 4.60%.

E(Z)-3-(2,4-dimethoxyphenyl)-2-(3-phenyl-3H-imidazo[4,5-b]pyridin-2-yl)acrylonitrile ***21***

21 was prepared from **9** (0.07 g, 0.30 mmol) and 15 (0.07 g, 0.30 mmol) in absolute ethanol (2 mL) after refluxing for 1.5 hours to yield 0.08 g (51%) yellow powder; m.p. 176-182 °C in the form of a mixture of *E*- and *Z*- isomers in the ratio 21a:21b = 10:1; 21a: ^1H NMR (400 MHz, DMSO) (δ/ppm): 8.34 (dd, J_1 = 4,7 Hz, J_2 = 1,5 Hz 1H, H_{arom}), 8.23 (dd, J_1 = 8.0 Hz, J_2 = 1.5 Hz, 1H, H_{arom}), 8.14 (d, J = 8.9 Hz, 1H, H_{arom}), 8.02 (s, 1H, CH), 7.65 – 7.58 (m, 5H, H_{arom}), 7.41 (dd, J_1 = 8.0 Hz, J_2 = 4.7 Hz, 1H, H_{arom}), 6.72 (dd, J_1 = 8.9 Hz, J_2 = 2.4 Hz, 1H, H_{arom}), 6.64 (d, J = 2.4 Hz, 1H, H_{arom}), 3.86 (s, 3H, OCH_3), 3.75 (s, 3H, OCH_3); 21b: ^1H NMR (400 MHz, DMSO) (δ/ppm): 8.39 (dd, J_1 = 4.7 Hz, J_2 = 1.5 Hz, 1H, H_{arom}), 8.26 (dd, 1H, J_1 = 8.02, J_2 = 1.46 Hz, H_{arom}), 7.78 (s, 1H, CH), 7.59 (s, 2H, H_{arom}), 7.44 (m, 2H, H_{arom}), 7.22 – 7.14 (m, 2H, H_{arom}), 6.41 (d, 1H, J = 2.34 Hz, H_{arom}), 6.38 (m, 1H, H_{arom}), 3.76 (s, 3H, OCH_3), 3.50 (s, 3H, OCH_3); APT ^{13}C NMR (101 MHz, DMSO) (δ/ppm): 165.00, 164.35, 160.78, 159.72, 149.75, 149.06, 147.90, 145.30 (2C), 145.30, 144.18 (2C), 135.04, 134.92, 134.61, 133.85, 131.24, 130.23 (2C), 129.77 (2C), 129.46, 129.35, 128.82 (2C), 128.69 (2C), 128.39, 127.66, 126.82, 120.16, 120.07, 118.55, 116.82, 114.22, 107.18, 106.68, 99.24, 98.77, 98.60, 97.06, 56.39, 56.27, 56.12, 56.05. MS (ESI): m/z= 318.18 ($[M+1]^+$). Anal. Calcd. For: $C_{23}H_{18}N_4O_2$: C, 72.24; H, 4.74; N, 14.65; O, 8.37. Found: C, 72.27; H, 4.70; N, 14.50; O, 8.40%.

(E)-2-(3-phenyl-3H-imidazo[4,5-b]pyridin-2-yl)-3-(3,4,5-trimethoxyphenyl)acrylonitrile ***22***

22 was prepared from **9** (0.07 g, 0.30 mmol) and 16 (0.07 g, 0.30 mmol) in absolute ethanol (2 mL) after refluxing for 1.5 hours to yield 0.09 g (52%) yellow powder; m.p. 166-168 °C; ^1H NMR (400 MHz, DMSO) (δ/ppm): 8.38 (dd, J_1 = 4.7 Hz, J_2 = 1.4 Hz, 1H, H_{arom}), 8.24 (dd, J_1 = 8.1 Hz, J_2 = 1.5 Hz, 1H, H_{arom}), 8.03 (s, 1H, CH), 7.65 – 7.60 (m, 5H, H_{arom}), 7.44 (dd, J_1 = 8.0 Hz, J_2 = 4.7 Hz, 1H, H_{arom}), 7.28 (s, 2H, H_{arom}), 3.79 (s, 6H, OCH_3), 3.76 (s, 3H, OCH_3); APT ^{13}C NMR (101 MHz, DMSO) (δ/ppm): 153.37 (2C), 151.71, 149.45, 148.37, 145.67, 141.55, 134.59, 134.55, 130.10, 129.89, 129.66, 128.69, 128.03, 127.90, 126.95, 120.32, 116.02, 108.12, 107.52, 99.24, 60.78, 56.47 (2C). MS (ESI): m/z= 413.17 ($[M+1]^+$). Anal. Calcd. For: $C_{24}H_{20}N_4O_3$: C, 69.89; H, 4.89; N, 13.58; O, 11.64. Found: C, 69.73; H, 4.92; N, 13.50; O, 11.55%.

(E)-3-(4-(dimethylamino)phenyl)-2-(3-phenyl-3H-imidazo[4,5-b]pyridin-2-yl)acrylonitrile ***23***

23 was prepared from **9** (0.07 g, 0.30 mmol) and 17 (0.07 g, 0.30 mmol) in absolute ethanol (2 mL) after refluxing for 1.5 hours to yield 0.09 g (87%) orange powder; m.p. 231-233 °C; ^1H NMR (400 MHz, DMSO) (δ/ppm): 8.31 (dd, J_1 = 4.7 Hz, J_2 = 1.4 Hz, 1H, H_{arom}), 8.17 (dd, J_1 = 8.0 Hz, J_2 = 1.4 Hz, 1H, H_{arom}), 7.76 – 7.71 (m, 3H, H_{arom}), 7.64 – 7.57 (m, 5H, H_{arom}), 7.39 (dd, J_1 = 8.0 Hz, J_2 = 4.7 Hz, 1H, H_{arom}), 6.79 (d, J = 9.1 Hz, 2H, H_{arom}), 3.05 (s, 6H, CH_3); APT ^{13}C NMR (101 MHz, DMSO) (δ/ppm): 153.29, 151.11, 149.88, 149.67, 144.77, 135.05, 134.74, 132.73 (2C), 132.58, 130.05, 129.67, 128.71, 127.27, 127.19, 119.95, 119.89, 117.44,

112.14, 111.93, 91.67, 40.04 (2C). MS (ESI): m/z= 366.17 ($[M+1]^+$). Anal. Calcd. For: $C_{23}H_{19}N_5$: C, 75.59; H, 5.24; N, 19.16. Found: C, 75.65; H, 5.24; N, 19.17%.

(E)-3-(4-(diethylamino)phenyl)-2-(3-phenyl-3H-imidazo[4,5-b]pyridin-2-yl)acrylonitrile ***24***

24 was prepared from **9** (0.07 g, 0.30 mmol) and 18 (0.07 g, 0.30 mmol) in absolute ethanol (2 mL) after refluxing for 1.5 hours to yield 0.10 g (59%) red powder; m.p. 231-233 °C; ^{1}H NMR (400 MHz, DMSO) (δ/ppm): 8.30 (dd, J_1 = 4.7 Hz, J_2 = 1.4 Hz, 1H, H_{arom}), 8.16 (dd, J_1 = 8.0 Hz, J_2 = 1.4 Hz, 1H, H_{arom}), 7.73 – 7.69 (m, 3H, H_{arom}), 7.60 (m, 5H, H_{arom}), 7.38 (dd, J_1 = 8.0 Hz, J_2 = 4.8 Hz, 1H, H_{arom}), 6.77 (d, J = 9.2 Hz, 2H, H_{arom}), 3.44 (q, J = 7.0 Hz, 4H, CH_2), 1.12 (t, J = 7.0 Hz, 6H, CH_3); APT ^{13}C NMR (101 MHz, DMSO) (δ/ppm): 151.06, 150.94, 150.04, 149.68, 145.92, 144.69, 135.09, 134.77, 133.14, 133.00, 130.04, 129.64, 128.69, 127.26, 127.11, 119.92, 119.33, 117.57, 111.73, 111.47, 90.94, 44.45 (2C), 12.87 (2C). MS (ESI): m/z= 394.22 ($[M+1]^+$). Anal. Calcd. For: $C_{25}H_{23}N_5$: C, 76.31; H, 5.89; N, 17.80. Found: C, 76.40; H, 5.95; N, 17.67%.

E(Z)-2-(3-isobutyl-3H-imidazo[4,5-b]pyridin-2-yl)-3-phenylacrylonitrile ***25***

25 was prepared from **10** (0.05 g, 0.23 mmol) and **13** (0.07 g, 0.23 mmol) in absolute ethanol (2 mL) after refluxing for 1.5 hours to yield 0.04 g (60%) yellow powder; m.p. 176-178 °C in the form of a mixture of *E*- and *Z*- isomers in the ratio 25a:25b = 3:1; 25a: ^{1}H NMR (400 MHz, DMSO) (δ/ppm): 8.46 (dd, J_1 = 4.7 Hz, J_2 = 1.5 Hz, 1H, H_{arom}), 8.41 (s, 1H, CH), 8.18 (dd, J_1 = 8.1 Hz, J_2 = 4.5 Hz, 1H, H_{arom}), 8.07 (m, 3H, H_{arom}), 7.39 (dd, J_1 = 8.0 Hz, J_2 = 4.7 Hz, 1H, H_{arom}) 4.45 (d, J = 7.6 Hz, CH_2), 2.28 (m, 1H, CH), 0.84 (d, 6H, J = 6.6 Hz, CH_3); 25b: ^{1}H NMR (400 MHz, DMSO) (δ/ppm): 8.48 (dd, J_1 = 4.8 Hz, J_2 = 1.5 Hz, 1H, H_{arom}), 8.27 (s, 1H, CH), 8.23 (dd, J_1 = 8.1 Hz, J_2 = 1.4 Hz, 1H, H_{arom}), 7.43 (m, 2H, H_{arom}), 7.34 (m, 2H, H_{arom}), 7.11 (m, 1H, H_{arom}), 3.75 (d, J = 7.6 Hz, 2H, CH_2), 2.20 (m, 1H, CH), 0.75 (d, J = 6.7 Hz, 6H, CH_3); APT ^{13}C NMR (151 MHz, DMSO) (δ/ppm): 152.20, 150.72, 148.93, 148.15, 147.75, 147.40, 147.05, 145.25, 145.12, 141.00, 135.38, 134.28, 133.01, 132.76, 131.40, 130.73, 130.40, 130.05, 129.76, 127.84, 127.67, 119.74, 119.66, 117.11, 116.85, 116.82, 101.20, 100.74, 50.23, 50.10, 48.26, 48.04, 29.32, 27.87, 20.07 (2C), 20.02 (2C). MS (ESI): m/z= 303.20 ($[M+1]^+$). Anal. Calcd. For: $C_{19}H_{18}N_4$: C, 75.47; H, 6.00; N, 18.53. Found: 75.40; H, 5.99; N, 18.42%.

(E)-2-(3-isobutyl-3H-imidazo[4,5-b]pyridin-2-yl)-3-(2-methoxyphenyl)acrylonitrile ***26***

26 was prepared from **10** (0.05 g, 0.23 mmol) and **14** (0.03 g, 0.23 mmol) in absolute ethanol (2 mL) after refluxing for 1.5 hours to yield 0.06 g (85%) yellow oil; ^{1}H NMR (600 MHz, DMSO) (δ/ppm): 8.55 (s, 1H, CH), 8.45 (dd, J_1 = 4.71 Hz, J_2 = 1.29 Hz, 1H, H_{arom}), 8.17 (dd, J_1 = 4.71 Hz, J_2 = 1.29 Hz, 1H, H_{arom}), 8.13 (dd, J_1 = 7.8 Hz, J_2 = 1.3 Hz, 1H, H_{arom}), 7.61 (t, J = 8.0, 1H, H_{arom}), 7.38 (dd, J_1 = 8.0 Hz, J_2 = 4.7 Hz, 1H, H_{arom}), 7.24 (d, J = 8.4 Hz, 1H, H_{arom}), 7.18 (t, J = 7.6 Hz, 1H. H_{arom}), 4.43 (d, J = 7.6 Hz, 2H, CH_2), 3.93 (s, 3H, OCH_3), 2.29 (m, 1H, CH), 0.86 (d, J = 6.56 Hz, 6H, OCH_3); APT ^{13}C NMR (151 MHz, DMSO) (δ/ppm): 158.74, 149.01, 148.18, 146.70, 145.15, 134.55, 134.26, 128.68, 127.77, 121.63, 121.22, 119.70, 116.83, 112.46, 101.17, 56.50, 50.10, 29.38, 20.07 (2C). MS (ESI): m/z= 332.90 ($[M+1]^+$). Anal. Calcd. For: $C_{20}H_{20}N_4O$: C, 72.27; H, 6.06; N, 16.86; O, 4.81. Found: C, 72.12; H, 6.02; N, 16.71; O, 4.84%.

E(Z)-3-(2,4-dimethoxyphenyl)-2-(3-isobutyl-3H-imidazo[4,5-b]pyridin-2-yl)acrylonitrile ***27***

27 was prepared from 10 (0.05 g, 0.23 mmol) and **15** (0.04 g, 0.23 mmol) in absolute ethanol (2 mL) after refluxing for 1.5 hours to yield 0.06 g (72%) yellow powder; m.p. 123-129 °C in the form of a mixture of *E*- and *Z*- isomers in the ratio 27a:27b = 3:1; 27a: ^{1}H NMR (600 MHz, DMSO) (δ/ppm): 8.51 (s, 1H, CH), 8.41 (dd, J_1 = 4.7 Hz, J_1 = 1.4 Hz, 1H, H_{arom}), 8.23 (d, J = 8,8 Hz, 1H, H_{arom}), 8.13 (dd, J_1 = 8.0 Hz, J_2 = 1.4 Hz, 1H, H_{arom}), 7.35 (dd, J_1 = 8.0 Hz, J_2 = 4.7 Hz, 1H, H_{arom}), 6.80 (dd, J_1 = 8.8 Hz, J_2 = 2.3 Hz, 1H, H_{arom}), 6.75 (d, J = 2.3 Hz, 1H, H_{arom}), 4.42 (d, J = 7.6 Hz, 2H, CH_2), 3.93 (s, 6H, OCH_3), 3.90 (s, 6H, OCH_3), 2.29-2,27 (m, 1H, CH), 0.85 (d, J = 6.7 Hz, 6H, CH_3), 27b: ^{1}H NMR (600 MHz, DMSO) (δ/ppm): 8.44 (dd, J_1 = 4.7 Hz, J_2 = 1.4 Hz, 1H, H_{arom}), 8.19 (dd, J_1 = 8.1 Hz, J_2 = 1.4 Hz, 1H, H_{arom}), 8.07 (s, 1H, CH), 7.39 (dd, J_1 = 8.0 Hz, J_2 = 4.7 Hz, 1H, H_{arom}), 6.65 (d, J = 2.3 Hz, 1H, H_{arom}), 6.56 (d, J = 8.9 Hz, 1H, H_{arom}), 6.36 (dd, J_1 = 8.8 Hz, J_2 = 2.3 Hz, 1H, H_{arom}), 3.80 (s, 3H, OCH_3), 3.76 (s, 3H, OCH_3), 3.74 (m, 2H, CH_2), 2.18-2.17 (m, 1H, CH), 0.75 (d, J = 6.7 Hz, 6H, CH_3); APT ^{13}C NMR (151 MHz, DMSO) (δ/ppm): 165.10, 164.67, 160.96, 160.27, 149.12, 148.85, 147.98, 147.03, 146.35, 145.45, 145.43, 144.75, 134.82, 134.30, 130.36 (2C), 129.81 (2C), 128.22, 127.42, 119.54, 118.95, 117.62, 114.48, 114.42, 107.20, 107.14, 98.96, 98.93, 98.34, 96.70, 56.70, 56.65, 56.32, 56.14, 50.18, 50.00, 29.38, 28.70, 20.08, 20.06 (2C). MS (ESI): m/z= 363.19 ($[M+1]^+$). Anal. Calcd. For: $C_{21}H_{22}N_4O_2$: C, 69.59; H, 6.12; N, 15.46; O, 8.83. Found: C, 69.50 H, 6.09; N, 15.37; O, 8.81%.

E(Z)-2-(3-isobutyl-3H-imidazo[4,5-b]pyridin-2-yl)-3-(3,4,5-trimethoxyphenyl)acrylonitrile ***28***

28 was prepared from **10** (0.05 g, 0.23 mmol) and **16** (0.04 g, 0.23 mmol) in absolute ethanol (2 mL) after refluxing for 1.5 hours to yield 0.06 g (72%) yellow crystals; m.p. 111-115 °C in the form of a mixture of *E*- and *Z*- isomers in the ratio 28a:28b = 3:1; 28a:^{1}H NMR (400 MHz, DMSO) (δ/ppm): 8.45 (dd, J_1 = 4.7 Hz, J_2 = 1.4 Hz, 1H, H_{arom}), 8.37 (s, 1H, CH), 8,15 (dd, J_1 = 8.0 Hz, J_2 = 1.5 Hz, 1H, H_{arom}), 7.52 (s, 2H, H_{arom}), 7.38 (dd, J_1 = 8.0 Hz, J_2 = 4.8 Hz, 1H, H_{arom}), 4.45 (d, J = 7.2 Hz, 2H, CH_2), 3.87 (s, 6H, CH_3), 3.80 (s, 3H, OCH_3), 2.25 (m, 1H, CH), 0.84 (d, J = 6.64 Hz, 6H, CH_3); 28b:^{1}H NMR (400 MHz, DMSO) (δ/ppm): 8.49 (dd, J_1 = 4.7 Hz, J_2 = 1.4 Hz, 1H, H_{arom}), 8.24 (dd, J_1 = 8.1 Hz, J_2 = 1.4 Hz, 1H, H_{arom}), 8,13 (s, 1H, CH), 7,42 (dd, J_1 = 8.1 Hz, J_2 = 4.7 Hz, 1H, H_{arom}), 3.84 (d, J = 7.5 Hz, 2H, CH_2), 3.65 (s, 3H, OCH_3), 3.32 (s, 6H, OCH_3), 2.24 (m, 1H, CH), 0.79 (d, J = 6.68, 6H, CH_3). APT ^{13}C NMR (151 MHz, DMSO) (δ/ppm): 153.43, 153.12, 152.79, 151.97 (2C), 149.02, 148.30, 147.68, 145.33, 145.09, 141.59, 134.29, 128.39, 128.21, 127.64 (2C), 127.46 (2C), 126.36, 119.71, 117.48, 117.27, 117.02, 108.42 (2C), 107.80 (2C), 100.15, 98.91, 60.80, 60.67, 56.53 (2C), 55.75 (2C), 50.22, 50.03, 30.32, 29.36, 20.06 (2C), 19.70 (2C). MS (ESI): m/z= 392.75 ($[M+1]^+$). Anal. Calcd. For: $C_{22}H_{24}N_4O_3$: C, 67.33; H, 6.16; N, 14.28; O, 12.23. Found: C, 67.07; H, 6.12; N, 14.34; O, 12.18%

E(Z)-3-(4-(dimethylamino)phenyl)-2-(3-isobutyl-3H-imidazo[4,5-b]pyridin-2-yl)acrylonitrile ***29***

29 was prepared from **10** (0.05 g, 0.23 mmol) and **17** (0.04 g, 0.23 mmol) in absolute ethanol (2 mL) after refluxing for 1.5 hours to yield 0.07 g (87%) yellow powder m.p. 125-129 °C in the form of a mixture of *E*- and *Z*- isomers in the ratio 29a:29b = 4:1; 29a:^{1}H NMR (600 MHz, DMSO) (δ/ppm): 8.37 (dd, J_1 = 4.7 Hz, J_2 = 1.4 Hz, 1H, H_{arom}), 8.19 (s, 1H, CH), 8.07 (dd, J_1 = 8.0 Hz, J_2 = 1.4 Hz, 1H, H_{arom}), 7.99 (d, J = 6.1 Hz, 2H, H_{arom}),

7.32 (dd, J_1 = 8.0 Hz, J_2 = 4.7 Hz, 1H, H_{arom}), 6.87 (d, J= 9,1 Hz, 2H, H_{arom}), 4.42 (d, J = 7.6 Hz, 2H, H_{arom}), 3.08 (s, 6H, CH_3), 2.29 – 2.20 (m, 1H, CH), 0.82 (d, J = 6.7 Hz, 6H, CH_3); 29b: ^{1}H NMR (600 MHz, DMSO) (δ/ppm): 8.46 (dd, J_1 = 4.8 Hz, J_2 = 1.5 Hz, 1H, H_{arom}), 8.20 (d, J = 1.4 Hz, 1H, H_{arom}), 7.90 (s, 1H, CH), 7.40 (dd, J_1 = 8.1 Hz, J_2 = 4.8 Hz, 1H, H_{arom}), 6.89 (d, J = 9.12 Hz, 2H, H_{arom}), 6.58 (d, J=9,2 Hz, $H_{arom, 2H}$), 3.85 (d, J = 7.6 Hz, 2H, CH_2), 3.34 (m, 4H, CH_2) 2.95 (s, 6H, CH_3), 2.29 – 2.20 (m, 1H, CH), 0.78 (d, J = 6.7 Hz, 6H, CH_3); APT ^{13}C NMR (151 MHz, DMSO) (δ/ppm): 153.38, 152.89, 151.93, 151.70, 149.70, 149.19, 148.04, 147.53, 145.32, 144.23, 134.95, 134.43, 133.02 (2C), 132.43 (2C), 128.19, 126.92, 120.17, 119.80, 119.76, 119.46, 119.33, 118.63, 112.18 (2C), 112.03 (2C), 92.79, 90.96, 50.27, 49.87, 40.11 (2C), 40.07 (2C), 29.27, 28.75, 20.15 (2C), 20.06 (2C). MS (ESI): m/z= 345.91 ($[M+1]^+$). Anal. Calcd. For: $C_{21}H_{23}N_5$: C, 73.02; H, 6.71; N, 20.27. Found: C, 72.88; H, 6.83; N, 20.21%.

E(Z)-3-(4-(diethylamino)phenyl)-2-(3-isobutyl-3H-imidazo[4,5-b]pyridin-2-yl)acrylonitrile ***30***

30 was prepared from **10** (0.06 g, 0.28 mmol) and **18** (0.05 g, 0.28 mmol) in absolute ethanol (2 mL) after refluxing for 1.5 hours to yield 0.04 g (41%) red crystals; m.p. 166-168 °C in the form of a mixture of *E*- and *Z*- isomers in the ratio 30a:30b = 3:1; 30a: ^{1}H NMR (600 MHz, DMSO) (δ/ppm): 8.36 (dd, J_1 = 4.7 Hz, J_2 = 1.4 Hz, 1H, H_{arom}), 8.15 (s, 1H, CH), 8.06 (d, J = 8.0 Hz, 1H, H_{arom}), 7.97 (d, J = 9.0 Hz, 2H, H_{arom}), 7.32 (dd, J_1 = 8.0 Hz, J_2 = 4.7 Hz, 1H, H_{arom}), 6.84 (d, J = 9.0 Hz, 1H, H_{arom}), 4.41 (d, J = 7.6 Hz, 2H, CH_2), 3.48 (q, J = 7.0 Hz, 4H, CH_2), 2.24 (m, 1H, CH), 1.15 (t, J = 7.0 Hz, 6H, CH_3), 0.82 (d, J = 6.7 Hz, 6H, CH_3); 30b: ^{1}H NMR (600 MHz, DMSO) (δ/ppm): 8.46 (d, J = 4.7 Hz, 1H, H_{arom}), 8.18 (d, J = 8.0 Hz, 1H, H_{arom}), 7.85 (s, 1H, CH), 7.39 (dd, J_1 = 8.0 Hz, J_2 = 4.7 Hz, 1H, H_{arom}), 6.87 (d, J = 8.94 Hz, 2H, H_{arom}), 6.55 (d, J = 9.0 Hz, 2H, H_{arom}), 3.88 (d, J = 7.6 Hz, 2H, CH_2), 3.34 (m, 1H, CH), 1.02 (t, J = 7.0 Hz, 6H, CH_3), 0.78 (d, J = 6.6 Hz, 6H, CH_3); APT ^{13}C NMR (151 MHz, DMSO) (δ/ppm): 151.53, 151.15, 149.85, 149.21, 144.15, 134.45, 133.43 (2C), 132.88 (2C), 128.16, 126.84, 119.61, 119.30, 118.77, 111.77 (2C), 92.67, 111.56 (2C), 90.20, 50.30, 49.86, 44.49 (2C), 44.22 (2C), 29.24, 28.76, 20.18 (2C), 20.06 (2C), 12.91 (2C), 12.80 (2C). MS (ESI): m/z= 374.29 ($[M+1]^+$). Anal. Calcd. For: $C_{23}H_{27}N_5$: C, 73.96; H, 7.29; N, 18.75. Found: C, 73.78; H, 7.21; N, 18.69%.

(E)-3-(4-(dimethylamino)phenyl)-2-(3-methyl-3H-imidazo[4,5-b]pyridin-2-yl)acrylonitrile ***31***

31 was prepared from **11** (0.07 g, 0.35 mmol) and **17** (0.06 g, 0.35 mmol) in absolute ethanol (2 mL) after refluxing for 1.5 hours to yield 0.04. g (31%) red powder; m.p. 128-129 °C; ^{1}H NMR (600 MHz, DMSO) (δ/ppm): 8.38 (dd, J_1 = 4.7 Hz, J_2 = 1.4 Hz, 1H, H_{arom}), 8.09 (s, 1H, CH), 8.07 (dd, J_1 = 8.0 Hz, J_2 = 1.4 Hz, 1H, H_{arom}), 8.00 (d, J = 9.1 Hz, 2H, H_{arom}), 7.33 (dd, J_1 = 8.0 Hz, J_2 = 4.7 Hz, 1H, H_{arom}), 6.88 (d, J = 9.1 Hz, 2H, H_{arom}), 4.02 (s, 3H, CH_3), 3.09 (s, 6H, CH_3); APT ^{13}C NMR (151 MHz, DMSO) (δ/ppm): 153.29, 151.03, 150.48, 149.07, 144.16, 134.74, 132.92 (2C), 126.81, 120.20, 119.23, 118.63, 112.14 (2C), 91.56, 40.07 (2C), 30.56. MS (ESI): m/z= 304.15 ($[M+1]^+$). Anal. Calcd. For: $C_{18}H_{17}N_5$: C, 71.27; H, 5.65; N, 23.09. Found: C, 71.35; H, 5.59; N, 22.97%.

E(Z)-3-(4-(diethylamino)phenyl)-2-(3-methyl-3H-imidazo[4,5-b]pyridin-2-yl)acrylonitrile ***32***

32 was prepared from **11** (0.07 g, 0.35 mmol) and **18** (0.07 g, 0.35 mmol) in absolute ethanol (2 mL) after refluxing for 1.5 hours to yield 0.02 g (17%) red crystals; m.p. 124-126°C in the form of a mixture of *E*- and *Z*- isomers in the ratio 32a:32b = 10:1; 32a: ^{1}H NMR (600 MHz, DMSO) (δ/ppm): 8.37 (dd, J_1 = 4.71 Hz, J_2 = 1.41 Hz, 1H, H_{arom}), 8.06 (s, 1H, CH) 8.05 (dd, J_1 = 7,9 Hz, J_2 = 1.4 Hz, 1H, H_{arom}), 7.97 (d, J = 9,1 Hz, 2H, H_{arom}), 7.31 (dd, J_1 = 7.9 Hz, J_2 = 4.7 Hz, 1H, H_{arom}), 6.84 (d, J = 9.2 Hz, 2H, H_{arom}), 4.01 (s, 3H, CH_3), 3,34 (m, 4H, CH_2) 1.15 (t, J = 7.1 Hz, 6H, CH_3); 32b: ^{1}H NMR (600 MHz, DMSO) (δ/ppm): 8.46 (dd, J_1 = 4.7 Hz, J_2 = 1.4 Hz, 1H, H_{arom}), 8.17 (dd, J_1 = 8.0, J_2 = 1.4 Hz, 1H, H_{arom}), 7.90 (s, 1H, CH), 7.39 (dd, J_1 = 8.0 Hz, J_2 = 4.8 Hz, 1H, H_{arom}), 6.91 (d, J = 9.1 Hz, 2H, H_{arom}), 6.56 (d, J = 9.2 Hz, 2H H_{arom}), 3.57 (s, 3H, CH_3), 3.34 (m, 4H, CH_2), 1.02 (t, J = 7.0 Hz, 6H, CH_3); APT ^{13}C NMR (151 MHz, DMSO) (δ/ppm): 151.07, 150.92, 150.61, 149.08, 144.07, 134.74, 133.34 (2C), 126.71, 119.63, 119.20, 118.76, 111.73 (2C), 90.71, 44.46 (2C), 30.55, 12.91 (2C). MS (ESI): m/z= 332.14 ($[M+1]^+$).Anal. Calcd. For: $C_{20}H_{21}N_5$: C, 72.48; H, 6.39; N, 21.13. Found: C, 72.27; H, 6.45; N, 21.02%.

(E)-3-(4-(dimethylamino)phenyl)-2-(3H-imidazo[4,5-b]pyridin-2-yl)acrylonitrile ***33***

33 was prepared from **12** (0.1 g, 0.63 mmol) and **17** (0.1 g, 0.63 mmol) in absolute ethanol (5 mL) after refluxing for 1.5 hours to yield 0.09 g (46%) orange powder; m.p. 189-192 °C; ^{1}H NMR (600 MHz, DMSO) (δ/ppm): 13.20 (bs, 1H, NH), 8.39 – 8.27 (m, 1H, H_{arom}), 8.21 (m, 1H, H_{arom}), 8.06 – 7.87 (m, 3H, H_{arom}), 7.26 – 7.20 (m, 1H, H_{arom}), 6.88 (d, J = 9.06 Hz, 2H, H_{arom}), 3.08 (s, 6H, CH_3); APT ^{13}C NMR (151 MHz, DMSO) (δ/ppm): 153.14, 149.55, 147.37, 147.04, 144.58, 144.29, 132.62, 126.49, 120.05, 118.64, 118.07, 117.88, 112.30 (2C), 94.07, 40.07 (2C). MS (ESI): m/z= 290.20 ($[M+1]^+$). Anal. Calcd. For: $C_{17}H_{15}N_5$: C, 70.57; H, 5.23; N, 24.20. Found: C, 70.69; H, 5.19; N, 24.29%.

E(Z)-3-(4-(diethylamino)phenyl)-2-(3H-imidazo[4,5-b]pyridin-2-yl)acrylonitrile ***34***

34 was prepared from **12** (0.1 g, 0.63 mmol) and **18** (0.09 g, 0.63 mmol) in absolute ethanol (5 mL) after refluxing for 1.5 hours to yield 0.1 g (57%) in the form of a mixture of *E*- and *Z*- isomers in the ratio 34a:34b = 10:1 as red crystals; m.p. 225-227 °C; 34a: ^{1}H NMR (600 MHz, DMSO) (δ/ppm): 13.40 (bs, 1H, NH), 8.38 – 8.16 (m, 2H, H_{arom}), 8.03 – 7.86 (m, 3H, H_{arom}), 7.24 (m, 1H, H_{arom}), 6.85 (d, J = 9.1 Hz, 2H, H_{arom}), 3.47 (q, J = 7.0 Hz, 4H, CH_2), 1.15 (t, J = 7.0 Hz, 6H, CH_3); 34b: ^{1}H NMR (600 MHz, DMSO) (δ/ppm): 12.97 (bs, 1H, NH), 8,50-8.44 (m, 2H, H_{arom}), 7.01 (m, 2H, H_{arom}), 6.64-6.58 (m, 1H, H_{arom}), 6.39 (d, J = 8.9 Hz, 1H, H_{arom}), 3.44 (m, 4H. CH_2), 1.06 (t, J = 7.0 Hz, 6H, CH_3); ^{13}C NMR (151 MHz, DMSO) (δ/ppm): 151.01, 150.91, 149.58, 147.22 (2C), 146.90 (2C), 144.54, 144.17, 135.99, 133.20 (2C), 133.04 (2C), 127.66, 126.39, 119.48 (2C), 119.36, 118.61, 118.50, 118.20, 118.01, 111.87 (4C), 93.33, 92.37, 44.47 (2C), 43.87 (2C), 12.91 (2C), 12.69 (2C). MS (ESI): m/z= 318.18 ($[M+1]^+$). Anal. Calcd. For: $C_{19}H_{19}N_5$: C, 71.90; H, 6.03; N, 22.07. Found: C, 72.14; H, 5.98; N, 22.15%.

2.2. ANTIOXIDATIVE POTENTIAL

Determination of the reducing activity of the DPPH radical

The reducing activity of investigated systems was achieved by the DPPH (1,1-diphenyl-picrylhydrazyl) method according to previously described procedures with modifications to assure the use in a 96-well microplate. Briefly, equal volumes of various concentrations of tested molecules (dissolved in DMSO) were added to the solution of DPPH (final concentration 50 μM in absolute ethanol). Ethanol and DMSO were used as control solutions in line with earlier reports [6,15,16].

Determination of Ferric Reducing/Antioxidant Power (FRAP assay)

The FRAP method was carried out according to previously described procedures [6] with some modifications to be compatible with an assay on a 96-well microplate. All results were expressed as Fe^{2+} equivalents (Fe^{2+} μmol). All tests were done in triplicate and the results were averaged [6].

ABTS Radical Scavenging Assay

The total antioxidant activity (TEAC) method [7] was modified and adjusted for the microtiter plate reader. For the standard TEAC assay, $ABTS^{\bullet+}$ (2,2′-azino-bis(3-ethylbenzothiazoline-6-sulfonic acid) radical cation was prepared by mixing an ABTS stock solution (7 mM in water) with 2.45 mM potassium persulfate, which was allowed to stand for 12–16 h at room temperature in the dark until reaching a stable oxidative state. On the day of analysis, the $ABTS^{\bullet+}$ solution was diluted with PBS (pH 7.4) to an absorbance of 0.700 ± 0.01 at 734 nm. The radical was stable in this form for more than two days when stored in the dark at room temperature. Standards and solutions of tested compounds (10 μL) were mixed with working $ABTS^{\bullet+}$ (200 μL) in microplate wells and incubated at room temperature for 5 min. The decrease of absorbance at 734 nm was recorded by μQuant (Biotec Inc.). Aqueous phosphate buffer solution and Trolox (0.20–1.25 mmol/L) were used as a control and a main calibrating standard, respectively. Results were expressed as average of three independent measure as trolox equivalents (mmol TEAC/ mmolC).

Determination of electrochemical oxidation potential

Electrochemical oxidation potentials of investigated compounds were determined using square-wave voltammetry (SWV). Voltammetric measurements were carried out using the computer-controlled electrochemical system “PGSTAT101” (Eco-Chemie, Utrecht, Netherlands) equipped with “NOVA 1.5” electrochemical software and a three-electrode system cell (BioLogic, Claix, France) with a glassy carbon electrode (GCE) of 3 mm in diameter as a working electrode, Ag/AgCl (3 mol L^{-1} NaCl) as a reference electrode and a platinum wire as a counter electrode. Before each run, the glassy-carbon working electrode was polished with diamond suspension in spray (grain size 6 μm) and rinsed with ethanol and deionised water. SWV responses were recorded in working solutions of compounds of interest ($c = 1x10^{-4}$ mol L^{-1}) obtained by diluting the stock solutions with the supporting electrolyte directly in the electrochemical cell. The supporting electrolyte was 0.6 M $NaClO_4$ (analytical grade; obtained from Kemika, Zagreb, Croatia) buffered to pH 3. Buffer solution was purchased from Reagecon (Shannon, Co. Clare, Ireland). SWV

conditions were: frequency, 100 Hz; square-wave amplitude, 50 mV; step potential, 2 mV. The solutions were degassed with high-purity nitrogen prior to the electrochemical measurements and a nitrogen blanket was maintained thereafter. Sqaure-wave voltammograms were taken in the potential scan range from –0.1 V to +1.6 V. All experiments were performed at room temperature.

2.3. COMPUTATIONAL DETAILS

As a good compromise between accuracy and feasibility, all of the molecular geometries were optimized with the density functional theory (DFT) using the B3LYP functional (unrestricted UB3LYP for the radicals), and the 6–31+G(d) basis set followed by the harmonic frequency calculations. Analysis of different conformations was done to select the most stable structures in each case. The thermal Gibbs free energy corrections were extracted from the corresponding frequency calculations without the application of scaling factors, while the obtained structures were confirmed as true minima by the absence of imaginary vibrational frequencies. To account for the solvation effects, we included the SMD polarizable continuum model with all parameters corresponding to pure ethanol (ε = 24.852), in accordance with presented experiments, giving rise to the (SMD)/B3LYP/6–31+G(d) model employed here. All reported values correspond to differences in Gibbs free energies obtained at a room temperature of 298 K and a normal pressure of 1 atm. The choice of this computational setup was prompted by its success in modeling mechanisms of various antioxidants [17–20], and in reproducing kinetic and thermodynamic parameters of a variety of organic and enzymatic reactions [21–24]. All calculations were performed using the Gaussian 16 software [25], while clogP values were estimated in ChemDraw Professional 15.0.

According to the literature, there are multiple mechanisms that relate the antioxidative properties of molecules [26–28]. In this work we evaluated the three most frequent, and usually thermodynamically most preferred antioxidant mechanisms, namely hydrogen atom transfer (HAT), related with the capacity to transfer the hydrogen atom ($H^{\bullet}$) to a free radical as governed by the M–H bond dissociation energy (BDE), and single electron transfer (SET) related with either ejecting or adding an electron to the system. All these mechanisms have the same net result, i.e. the formation of corresponding antioxidant radical and are calculated as Gibbs free energies for the following processes:

$$\mathbf{M}\text{–H} \rightarrow \mathbf{M}^{\bullet} + H^{\bullet} \quad \text{bond dissociation energy, BDE} = G(\mathbf{M}^{\bullet}) + G(H^{\bullet}) - G(\mathbf{M}\text{–H})$$

$$\mathbf{M} \rightarrow \mathbf{M}^{\bullet+} + e^{-} \quad \text{ionization energy, IE} = G(\mathbf{M}^{\bullet+}) + G(e^{-}) - G(\mathbf{M})$$

$$\mathbf{M} + e^{-} \rightarrow \mathbf{M}^{\bullet-} \quad \text{electron affinity, EA} = G(\mathbf{M}^{\bullet-}) - G(\mathbf{M}) - G(e^{-})$$

where the Gibbs free energy of an electron in ethanol solution, $G(e^{-})$, is taken from the literature [29].

3. RESULTS AND DISCUSSION

3.1. CHEMISTRY

The synthesis of novel *N*-substituted imidazo[4,5-b]pyridine derived acrylonitriles **19–34** is presented in Scheme 1. Starting from 2-chloro-3-nitropyridine **1**, due to the uncatalyzed microwave assisted amination in acetonitrile with an excess of methylamine, isobutylamine and aniline, N-substituted nitro precursors **2–4** were obtained in good reaction yields. To reduce the nitro group, we employed either Pd/C and ammonium formate [30,31] or $SnCl_2 \times 2H_2O$ to obtain diamino substituted precursors **5–7** in moderate yields. The main precursors, N-substituted 2-cyanomethylimidazo[4,5-b]pyridines **9–12** were prepared in the reaction of termic cyclocondensation with ethyl cyanoacetate at 185 °C in moderate reaction yields [32]. Due to the condensation of precursors **9–12** with chosen substituted aromatic benzaldehydes **13–18** in absolute ethanol with a few drops of piperidine, targeted acrylonitrile derivatives **19–34** were obtained in moderate yields after the purification by using column chromatography [33,34]. Some of the prepared acrylonitrile derivatives obtained as a mixture of *E*- and *Z*-isomers (**21**, **25**, **27–30**, **32** and **34**) and could not be efficiently separated by the column chromatography.

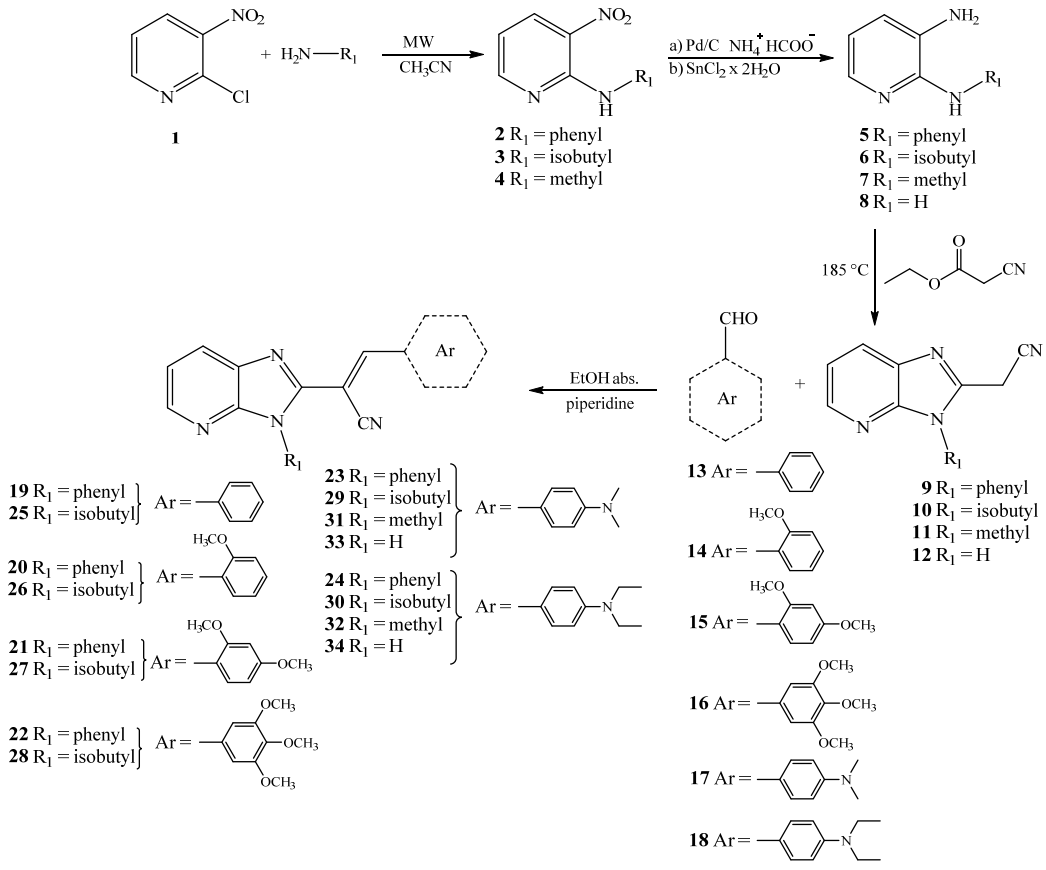

Scheme 1. Synthesis of imidazo[4,5-*b*]pyridine derived acrylonitriles **19–34**.

Table 1. ^{1}H NMR chemical shifts of some characteristic aromatic protons of **19**–**34**.

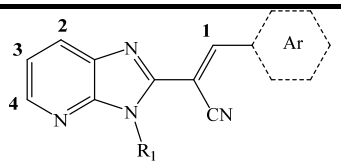

	^{1}H NMR (δ/ppm)			
System	**H-1**	**H-2**	**H-3**	**H-4**
19	7.94	8.27	7.45	8.39
20	8.04	8.27	7.44	8.37
21	8.02	8.23	7.41	8.34
22	8.03	8.24	7.44	8.38
23	7.70	8.17	7.39	8.31
24	7.70	8.16	7.38	8.30
25	8.41	8.18	7.39	8.46
26	8.55	8.17	7.38	8.45
27	8.51	8.13	7.35	8.41
28	8.37	8.15	7.38	8.45
29	8.19	8.07	7.32	8.37
30	8.15	8.06	7.32	8.36
31	8.09	8.07	7.33	8.38
32	8.06	8.05	7.31	8.37
33	7.96	8.26	7.24	8.32
34	7.94	8.24	7.24	8.29

The structures of all newly prepared acrylonitriles were characterized by ^{1}H and ^{13}C NMR spectroscopy, mass spectrometry and elemental analysis. The structure determination was performed based on the chemical shifts in both NMR spectra and values of H–H coupling constants in the ^{1}H spectra (Table 1). The amination reaction of reactant **1** was confirmed within the observation of the signals related to amino substituents in the aliphatic part (compounds **3–4**) and aromatic part (compound **5**) of both ^{1}H and ^{13}C NMR spectra. The signals for NH proton were placed in the range of 9.96-8.47 ppm. Furthermore, after the reduction of nitro precursors, in the ^{1}H spectra of compounds **5–7**, the signal of amino group was observed in the region of 5.06-4.59 ppm. The formation of 2-cyanomethylimidazo[4,5-*b*]pyridine derivatives **9–12** was confirmed with signals in the region of 4.61-4.42 ppm related to methylene group as well as with the disappearance of signals for amino groups. Singlet of acrylonitrile proton in the range from 8.55–7.70 ppm confirmed the formation of acrylonitrile derivatives **19**–**34**.

3.2. ANTIOXIDATIVE POTENTIAL OF PREPARED ACRYLONITRILES 19–34

To determine the antioxidant potency of newly prepared compounds, except system **20**, the radical scavenging capacity was measured against DPPH and ABTS stable radicals as well as through the ferric reducing ability/antioxidant power (FRAP) ability to reduce ferric to ferrous ion. Additionally, the electrochemical oxidation potential was measured. Results obtained using spectrophotometric assays were compared to a standard compound 3,5-di-tert-4-butylhydroxytoluene (BHT) in Tables 2 and 3.

Table 2. IC_{50} values of tested derivatives for DPPH and ABTS activities.

Cpd	DPPH IC50 / mM	ABTS IC50 / mM
19	0.47 ± 10^{-4}	$2.97 \pm 2\times10^{-4}$
25	$6.47 \pm 3\times10^{-4}$	$14.95 \pm 2\times10^{-4}$
26	$2.08 \pm 2\times10^{-4}$	$5.25 \pm 9\times10^{-4}$
BHT	0.025 ± 4.2	0.182 ± 0.02

DPPH approach is a broadly used spectroscopic radical scavenging method based on the ability of studied compounds to donate a proton or an electron to DPPH. $ABTS^{\bullet+}$ radicals are more reactive than DPPH radicals and could be used to evaluate hydrophilic and lipophilic compounds as well. The antioxidant capacity is measured as the ability of pure compounds to decrease the color reacting directly with the $ABTS^{\bullet+}$. The reducing power of tested compounds refers to their antioxidant activity and this method is based on the changes in the absorbance at 593 nm as a result of the ability of tested compounds to reduce the ferric tripyridyl triazine complex (TPTZ) to the ferrous state (Fe^{2+}) which may result in an intense blue color. Table 2 displays results obtained for DPPH and ABTS free radical scavenging features expressed as IC_{50} values, only for three derivatives which showed some activities. All other tested derivatives were not active at all in both methods. Evaluated systems were less active relative to standard BHT. The most promising radical scavenging activity was displayed by *N*-phenyl substituted derivative **19** with the unsubstituted phenyl ring.

Measured FRAP activities and electrochemical oxidation potentials for all tested derivatives are shown in Table 3. FRAP activities reveal that all tested compounds exhibit improved activity in comparison to standard antioxidant BHT with the exception of **25**, whose activity is similar to BHT. The most active derivatives were compounds substituted with the *N,N*-diethylamino group placed at the *para* position of phenyl ring bearing either phenyl (**24**), isobutyl (**30**), methyl (**32**) and H atom (**34**) at the N atom of imidazo[4,5-*b*]pyridine nuclei showing significantly improved activity when compared to a reference BHT. The most promising antioxidant activity was displayed by *N,N*-$(CH_3)_2$ substituted compound **29** bearing isobutyl side chain at the N atom of imidazo[4,5-*b*]pyridine nuclei (2485.5±4.2). Pronounced activity in comparison to standard BHT was also shown by *N,N*-$(CH_3)_2$ substituted compound **23** substituted with phenyl ring at N atom of imidazo[4,5-*b*]pyridine nuclei.

The logP value defined as 1-octanol/water partition coefficient is indicative for the lipophilicity or hydrophilicity of newly prepared compounds, which is very important for their possible penetration and crossing the cell membrane (Table 3). It appears that clogP values strongly depend on the type and number of substituents placed either on the imidazo[4,5-*b*]pyridine N-atom or within the phenyl ring. Thus, derivatives with *N,N*-dimethylamino (**23** and **29**) and *N,N*-diethylamino groups (**24** and **30**) on the phenyl moiety have higher clogP values relative to the methoxy substituted derivatives, which parallels their higher antioxidative activities. *N,N*-dimethylamino **23** and *N,N*-diethylamino **24** substituted systems with

the *N*-phenyl ring showed enhancement of clogP value when compared to *N*-isobutyl substituted analogues. Regarding the methoxy substituted derivatives bearing *N*-phenyl and *N*-isobuthyl groups, systems **22** and **28**, with three methoxy groups on the phenyl ring have decreased clogP values. Furthermore, the introduction of the *N*-methyl moiety (**31** and **32**) reduces clogP value in comparison to phenyl and isobutyl *N*-substituted analogues.

Table 3. FRAP activities, electrochemical oxidation potentials and clogP values for tested compounds.

Cpd	FRAP $mmolFe^{2+}/mmol_C$	E_a / V *vs*. Ag/AgCl (3M NaCl)	clogP
19	1124.5 ± 22.2	–	3.88
21	1239.2 ± 18.5	1.275	3.89
22	1134.6 ± 23.8	1.239	3.18
23	1955.9 ± 67.6	0.898	4.05
24	2119.1 ± 13.2	0.889	5.11
25	663.6 ± 15.8	–	3.26
26	1188.0 ± 72.9	–	3.18
27	1378.9 ± 10.0	1.285	3.26
28	1249.6 ± 18.5	1.256	2.56
29	2485.5 ± 4.2	0.876	3.42
30	2261.1 ± 16.4	0.909	4.48
31	831.0 ± 19.0	–	1.96
32	2365.6 ± 1.6	0.898	3.02
33	711.4 ± 13.7	–	2.14
34	2316.7 ± 61.3	0.626	3.20
BHT	679.15	–	–

Electrochemical methods, such as cyclic and square-wave voltammetry, are powerful tools for the analysis of antioxidant reactivity, because both the chemical reaction between antioxidant and the free radical and electrochemical oxidation of antioxidants involve the cleavage of the same O–H bond and the donation of electrons and protons [35]. In voltammetry, the main parameter used for evaluation of the antioxidant potential of a specific compound is the potential of the first oxidation wave/peak. To be more precise, compounds with less positive oxidation potential, i.e. higher susceptibility to electrochemical oxidation, possess a higher radical scavenging activity [36–38]. Indeed, reasonably good correlations have been obtained between electrooxidation peak potentials and spectrophotometrically determined radical scavenging activity for different compound groups, such as flavonoids [35,39,40], diarylamines [41] and indoles [42].

Here, we used the square-wave voltammetry to estimate the antioxidant activity of systems of interest based on the value of their electrochemical oxidation potentials. Nearly all tested compounds, except derivatives **19**, **25**, **26**, **31** and **33**, were oxidizable at the glassy-carbon electrode within the applied potential window. The results obtained for the square-wave voltammograms for the screened compounds

are shown in Table 2. System **34**, bearing *p*-*N,N*-$(CH_2CH_3)_2$ substituent on the distant phenyl moiety and lacking substituent at the N atom of imidazo[4,5-*b*]pyridine nuclei, had the lowest (least positive) oxidation potential (E_a = 0.626 V) and was most easily oxidized.

The *N*-substitution of the imidazo[4,5-*b*]pyridine ring, as in **24**, **32** and **30**, shifted the oxidation potential towards more positive values, around +0.250 V relative to the oxidation potential of **34** (meaning these compounds are more difficult to oxidize). When comparing compounds with identical substitution on the phenyl moiety but different type of substituent on the imidazo[4,5-*b*]pyridine nuclei, one can see that the latter did not significantly influence the oxidation potential (e.g. compare compounds **24**, **30** and **32** or compounds **22** and **28**). Replacement of *p*-*N,N*-$(CH_2CH_3)_2$ with *p*-*N,N*-$(CH_3)_2$ group had a negligible effect on oxidation potential. However, methoxy substitution on the phenyl moiety (**21**, **22**, **27** and **28**) shifted the oxidation peak potentials to high positive values, more positive than +1.2 V. By comparing oxidation potentials with the FRAP activity, the compounds with lower oxidation potentials were also more effective Fe^{3+} reducing agents. Moreover, linear correlation between electrooxidation potentials and FRAP activities yielded a correlation coefficient of r = 0.91 (Figure 2).

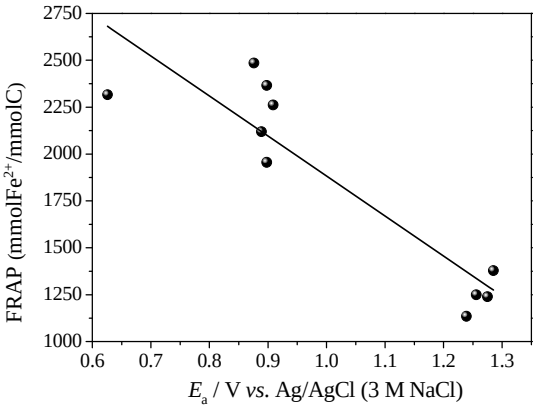

Figure 2. The relationship between electrochemical oxidation potential and FRAP activity of studied compounds.

3.3. COMPUTATIONAL ANALYSIS

Computational analysis was utilized to provide a further insight into the structure and properties of the examined systems and offer the interpretation of their antioxidant properties. Given a large number of structurally similar compounds evaluated here, we decided to address a selected number of derivatives, involving **19, 23**, **25, 31, 33, 34** and most potent **29**, together with several model systems **M1–M13** (Figure 3). The latter are selected to allow enough structural and electronic information about the studied compounds in order to aid in the design of even more potent antioxidants based on the employed organic framework. Results in Table 4 show that each system is characterized by its single-electron ionization energy (IE) and electron affinity (EA), together with the bond dissociation energy (BDE) required to homolytically cleave the hydrogen atom ($H^{\bullet}$) in thermodynamically most favorable way. In some

representative instances, this X–H cleavage is additionally described with the kinetic barrier ($\Delta G^{\ddagger}$) and the reaction free energy (ΔG_R) for the reaction with the hydroperoxyl radical ($HOO^{\bullet}$) that offers H_2O_2. Prior to going into details, we note that in most cases the antioxidative activity of experimentally evaluated systems is related with the donation of the hydrogen atom, seen in the least endegonic BDE values over IEs and EAs. This gives the preference to the hydrogen-abstraction mechanism, in line with our earlier results [17,18], which is why BDEs will be in focus throughout the discussion.

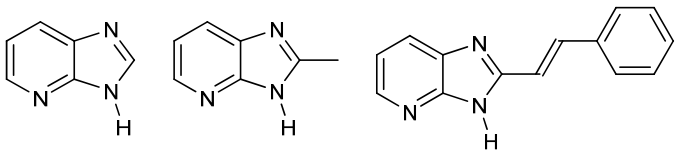

M1 **M2** **M3**

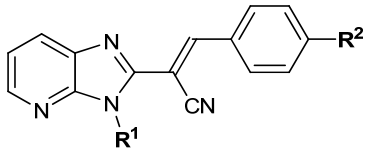

System	R^1	R^2	System	R^1	R^2	System	R^1	R^2
M4	H	H	**M8** (**33**)	H	$N(Me)_2$	**M12** (**34**)	H	$N(Et)_2$
M5	Me	H	**M9** (**31**)	Me	$N(Me)_2$	**M13**	Me	OMe
M6 (**25**)	*i*Bu	H	**M10** (**29**)	*i*Bu	$N(Me)_2$			
M7 (**19**)	Ph	H	**M11** (**23**)	Ph	$N(Me)_2$			

Figure 3. Chemical structures of systems evaluated computationally.

Table 4. Electron affinities (EAs), ionization energies (IEs) and bond dissociation energies (BDEs) in ethanol solution calculated at the (SMD)/B3LYP/6–31+G(d,p) level of theory. The corresponding position of the hydrogen atom abstraction is denoted next to a BDE value. Activation ($\Delta G^{\ddagger}$) and reaction (ΔG_R) free energies correspond to the hydrogen-transfer reaction with the $HOO^{\bullet}$ radical. All values are in kcal mol^{-1}.

System	EA	IE	BDE	Position	$\Delta G^{\ddagger}$	ΔG_R
M1	59.2	128.3	93.2	imidazole N–H	30.0	18.5
M2	57.5	123.3	80.9	imidazole methyl C–H	25.7	6.2
M3	76.5	110.4	82.7	imidazole N–H		
M4	88.6	117.3	84.3	imidazole N–H	24.9	8.1
M5	86.8	117.5	87.4	imidazole *N*-methyl C–H		
M6 (**25**)	86.8	117.5	83.5	imidazole *N*-isobutyl C–H	24.1	9.3
M7 (**19**)	87.3	119.4	90.6	alkene C–H	36.2	15.9
M8 (**33**)	81.7	100.4	78.2	imidazole N–H	15.4	3.5
M9 (**31**)	80.4	100.0	80.6	aniline *N*-methyl C–H	18.9	6.4
M10 (**29**)	79.1	101.2	80.6	aniline *N*-methyl C–H	18.3	5.5
M11 (**23**)	80.7	101.3	81.2	aniline *N*-methyl C–H	19.4	6.5
M12 (**34**)	82.2	99.6	77.0	aniline *N*-ethyl C(α)–H		
M13	84.1	111.7	86.5	imidazole *N*-methyl C–H		

The structure of studied systems depends on the location of a proton between imidazole N-atoms, for which 1*H*- and 3*H*-tautomers are probable, and on the orientation of different groups around the central double bond, for which *E*- and *Z*-isomers are possible. In all derivatives, the 3*H*-tautomer represents the most dominant structure, which turns more favorable than having two nitrogen lone-pairs vicinal to each other, as in 1*H*-analogues. In less substituted systems, the relative stability among tautomers is smaller, yet still making **M1**, **M2** and **M3** more stable as 3*H*-analogues by 0.1, 0.1 and 0.5 kcal mol^{-1}, respectively. In larger compounds, this increases to 1.1, 1.3 and 1.5 kcal mol^{-1} for **M8**, **M12** and **M4**, in the same order, thus confirming the prevalence of 3*H*-tautomers. Analogously, our calculations show that all investigated systems prefer *E*-isomers, being between 0.9 and 4.5 kcal mol^{-1} more stable than *Z*-alternatives (Table S1). Interestingly, for **M6** (**25**), **M10** (**29**) and **M12** (**34**) this assumes 0.9, 1.4 and 4.0 kcal mol^{-1}, respectively, which is found in excellent qualitative agreement with 3:1, 4:1 and 10:1 ratios determined experimentally (see Materials and Methods section), thus validating these calculations. Taken all together, all systems were considered as 3*H*-tautomers and *E*-isomers for the subsequent analysis, which agrees with our earlier reports on similar systems [8,17,18,34].

Investigated systems are based on the imidazo[4,5-*b*]pyridine derived acrylonitriles and the parent **M4** is linked with the BDE(**M4**) = 84.3 kcal mol^{-1}. To put this number in a proper context, let us mention that the measured value for a similar cyclic aromatic amine in iminostilbene assumes BDE = 82.4 ± 0.5 kcal mol^{-1} in the benzene solution [43], which places our value in the appropriate range and gives it credence. Also, if HOO$^{\bullet}$ is taken as a reference, this N–H cleavage is linked with a rather high kinetic requirement ($\Delta G^{\ddagger}$ = 24.9 kcal mol^{-1}) and a very much unfavorable ΔG_R = 8.1 kcal mol^{-1}, both making **M4** a weak antioxidant. It is followed by the acrylonitrile C–H moiety, yet its value of 93.7 kcal mol^{-1}, being 9.4 kcal mol^{-1} higher, clearly indicates that the antioxidative activity of **M4** exclusively pertains to the amine N–H position. If we further delineate this systems, it shows a higher antioxidative potential than the unsubstituted imidazo[4,5-*b*]pyridine skeleton **M1**, where the BDE is increased to 93.2 kcal mol^{-1}, together with a highly poor kinetic ($\Delta G^{\ddagger}$ = 30.0 kcal mol^{-1}) and thermodynamic aspects (ΔG_R = 18.5 kcal mol^{-1}) of the reaction with HOO$^{\bullet}$. The later justifies the use of the employed organic skeleton and verifies the presented design strategy as useful towards improved antioxidants. Interestingly, a simple extension of **M1** towards its 2-methyl derivative **M2** not only lowers the BDE by as much as 12.3 kcal mol^{-1} to BDE(**M2**) = 80.9 kcal mol^{-1}, but also changes the site of the homolytic cleavage to the introduced methyl group. This suggests that in carefully designed systems, the strength of the C–H bond can outperform the N–H bonds in terms of the hydrogen abstraction, which in **M2** assumes 93.7 kcal mol^{-1}, being similar to **M1**. The latter is also seen in the reactivity parameters, which are reduced to $\Delta G^{\ddagger}$(**M2**) = 25.7 kcal mol^{-1} and ΔG_R(**M2**) = 6.2 kcal mol^{-1} for the C–H abstraction, being consistently less favorable for the matching N–H bond with $\Delta G^{\ddagger}$ = 28.2 kcal mol^{-1} and ΔG_R = 16.0 kcal mol^{-1}.

To evaluate the effect of the attached –CN group, the calculated BDE for **M3** is by 1.6 kcal mol^{-1} lower than in **M4**, thus indicating that the nitrile group on the vinyl moiety diminishes the antioxidative features of the designed systems. However, the necessity of having the –CN group at this position stems from the employed synthetic approach, yet the attempts to prepare similar derivatives without it will be addressed in the future research. Still, the antioxidative capacity of **M4** can be significantly modulated by the *N*-substitution of the imidazo[4,5-*b*]pyridine unit as in **M5**–**M7**, which is particularly interesting knowing that, when present, the unsubstituted N–H bond is dominating the investigated properties. Interestingly, such a substitution only marginally modulates the calculated EA and IP parameters, yet the effect on the BDE values is larger. The introduced *N,N-*$(CH_3)_2$ (**M5**) makes it the site for the hydrogen abstraction, yet the calculated BDE is increased by 3.1 kcal mol^{-1} to BDE(**M5**) = 87.4 kcal mol^{-1}.

A much more favorable outcome is achieved with a larger *N*-isobutyl unit, where the hydrogen cleavage is most easily performed on the tertiary C-atom within the later, associated with BDE(**M6**) = 83.5 kcal mol^{-1}. This helps explain why *N*-isobutyl derivative **29** is the most potent antioxidant evaluated here, as, for example, its FRAP parameter is three times higher than in the analogous *N*-methyl system **31**. Contrary to that, placing the *N*-phenyl unit on the imidazo[4,5-*b*]pyridine core turns as a poor option. Specifically, in **M7** this is seen in making the alkene C–H bond as the site of the hydrogen abstraction, linked with the least favorable BDE = 90.6 kcal mol^{-1} and $\Delta G^{\ddagger}$ = 36.2 kcal mol^{-1} values and the second least favorable ΔG_R = 15.9 kcal mol^{-1} value of all studied systems, that jointly contribute towards its very limited antioxidative capacity. Experimentally this is seen in consistently lower FRAP values for **21**–**24** over their *N*-isobutyl analogues **27**–**30** (Table 2). Another route towards improved antioxidants is through introducing electron-donating substituents on the distant phenyl moiety, especially in the *para*-position. Dialkylamino groups are much better in this respect over their methoxy analogues, as, for example, **M9** has by 5.9 kcal mol^{-1} lower BDE value than **M13**, which is also observed in the related FRAP and electrooxidation potential values (Table 2). Along these lines, all *N*,*N*-dimethylamino systems **M8**–**M11** are better antioxidants than their unsubstituted **M4**–**M7** derivatives. Part of this effect stems from the fact that the introduced *N*,*N*-dimethylamino groups become the site for the hydrogen abstraction, thus prevailing over *N*-alkyl groups within the imidazo[4,5-*b*]pyridine core. It turns out that aniline nitrogens are more prone towards electron donation towards the vicinal carbon-centered radicals in **M8**–**M11** than are imidazole nitrogens in **M4**–**M7**, thus the better antioxidants in the former. Lastly, replacing the *p-N,N-*$(CH_3)_2$ group with a larger *p-N,N-*$(CH_2CH_3)_2$ moiety further promotes antioxidant features. This can be traced down either to a better electron-donating ability of the latter, which dominates when the hydrogen abstraction occurs somewhere else on the molecule, or to a fact that the cleavage of the C(α)–H bond within the diethylamino group experiences extra stabilization from the additional β-methyl group, not present in the dimethylamino unit. Both of these effects are seen in **M12**, which is by 1.2 kcal mol^{-1} a more potent antioxidant than related **M8**. Interestingly, in the former this corresponds to the hydrogen abstraction from the *N*-ethyl C(α)–H bond, yet the homolytic cleavage of the imidazole N–H group, analogous to that in **M8** is only 0.2 kcal mol^{-1}

less favorable (BDE = 77.2 kcal mol^{-1}), still surpassing by 1.0 kcal mol^{-1} the situation in the *p-N,N-*$(CH_3)_2$ derivative **M8**. With this in mind, it seems that introducing even more efficient electron-donating groups on the phenyl ring based on the amino functionality provides useful guidelines towards more prominent antioxidants, which will be tackled in future studies.

3.4. SPECTROSCOPIC CHARACTERIZATION

To study the spectroscopic properties of **24, 30, 32** and **34**, UV-Vis absorption spectra were recorded in several organic solvents with different polarity selected also to ensure good solubility of compounds (Table 5). Suchlike systems have proven to have excellent spectroscopic properties [44,45] that allowed them the potential use as sensitive and selective optical sensors in a wide range of biological, environmental, and chemical processes.

Table 5. Spectroscopic data for characterized derivatives.

Solvent	E_T (30)	24		30		32		34	
		λ_{max} (nm)	$\varepsilon \times 10^3$ ($dm^3mol^{-1}cm^{-1}$)	λ_{max} (nm)	$\varepsilon \times 10^3$ ($dm^3mol^{-1}cm^{-1}$)	λ_{max} (nm)	$\varepsilon \times 10^3$ ($dm^3mol^{-1}cm^{-1}$)	λ_{max} (nm)	$\varepsilon \times 10^3$ ($dm^3mol^{-1}cm^{-1}$)
Toluene	33.9	399	26.3	398	41.4	401	27.2	440	35.8
		326	4.4	325	6.1	324	4.4	322	6.3
		301	10.8	295	15.3	297	10.5	306	10.6
$(C_2H_5)_2O$	34.5	391	31.8	389	44.5	392	32.9	428	41.2
		323	4.9	322	6.5	324	4.6	325	5.0
		294	12.4	294	15.6	294	12.2	299	11.1
Dioxane	36.0	398	29.4	396	50.4	399	28.4	437	35.2
		325	4.5	326	6.6	323	4.5	325	4.8
		294	11.7	295	17.9	295	10.8	303	10.2
EtAc	38.1	397	29.9	395	43.7	398	30.6	434	34.1
		326	4.1	324	5.9	324	4.2	327	4.0
		294	11.4	294	15.8	300	11.0	303	9.8
CH_2Cl_2	40.7	407	29.5	405	45.5	410	30.3	447	38.0
		325	4.8	326	5.9	326	4.2	327	4.8
		298	11.2	295	15.2	298	10.9	304	11.4
CH_3CN	45.6	405	30.0	402	45.0	405	31.2	439	34.6
		324	4.5	330	4.1	324	4.2	326	4.4
		293	10.9	294	14.8	303	10.3	302	10.3
EtOH	51.9	407	29.3	407	44.7	410	30.6	449	32.8
		326	4.5	323	6.4	324	4.3	322	5.2
		294	10.9	293	15.1	294	11.1	302	10.5
MeOH	55.4	409	32.7	413	47.4	412	31.0	442	33.8
		326	5.0	323	6.4	324	4.4	322	5.4
		307	9.7	293	15.8	300	10.7	303	10.9
		292	11.9						
Water	63.1	422	25.6	413	30.5	419	28.2	456	31.4
		295	12.1	297	12.0	325	47.6	324	5.6
						295	10.5	304	10.6

In order to inspect the solvent effect on the spectroscopic characteristics of tested compounds, stock solutions were prepared in five polar and four non-polar solvents. UV-Vis spectra were measured in the range of 290–550 nm at the same concentration of 2×10^{-5} mol dm^{-3} at room temperature. The absorption spectra of all measured compounds (Figure 4 and Figure S53) showed one main absorption band in all solvents in the region between 300–550 nm.

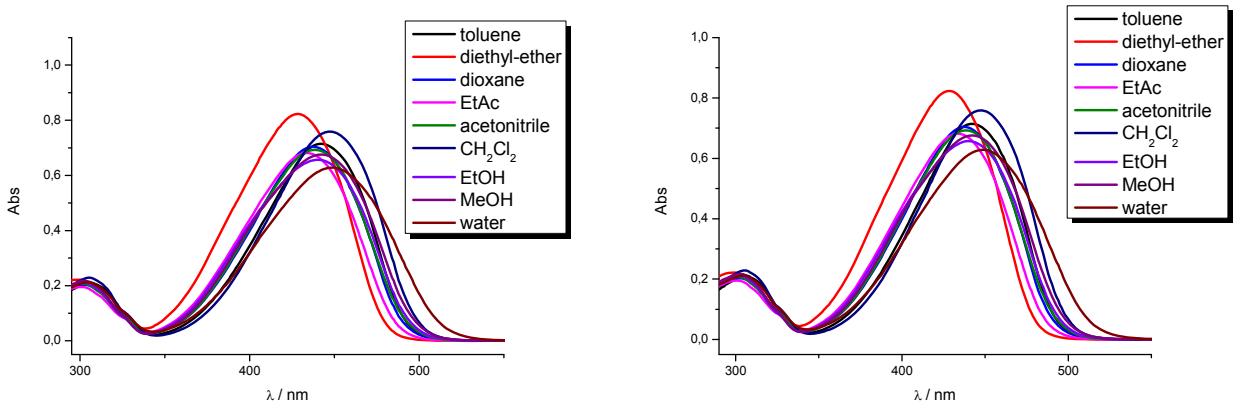

Figure 4. UV/Vis spectra of **24** (left) and **34** (right) at c ≈ 2 × 10^{-5} mol dm^{-3} in organic solvents of varying polarities.

Considering the absorption spectra of **24**, the most intensive absorbance with a slight hyperchromic effect and a slight bathochromic shift in comparison to all other solvents except water, was observed. Apart from the small bathochromic shift of maxima, in water **24** also showed the hypochromic effect. Non-polar solvents caused a slight hypsochromic shift of the absorbance maxima when compared to absorption spectra taken in polar solvents. System **30** showed the most intensive absorbance in dioxane with a hypsochromic shift of absorption maxima relative to polar solvents. In diethyl-ether, ethyl acetate and water we observed the hypochromic shift of absorption intensity, while in water and methanol there is a bathochromic shift of absorption maxima. System **32** showed the most intensive absorbance in diethyl-ether as well as **34**, and the lowest intensity in dichloromethane, while the most significant bathochromic shift of absorption maxima can be observed in water. Compound **34** display bathochromic shift of absorption maxima as well as hypochromic shift of absorption intensity in water. The recorded absorption spectra of examined compounds revealed that the polarity of solvents had the influence on the absorption maxima and intensity. Thus, the most significant bathochromic shift can be observed for all compounds in water, while the most significant hypsochromic shift is observed in diethyl-ether. Additionally, the hypochromic shift of absorption intensity is the highest in water for **24**, **30** and **34** when compared to all other used solvents.

Figure 5 shows the absorption spectra of several compounds in a non-polar dioxane and polar water. Based on these, we can conclude that the type of the substituent placed at the N atom of

imidazo[4,5-*b*]pyridine nuclei has a strong impact on the spectroscopic properties. In dioxane, **30** substituted with the isobutyl side chain showed the highest absorption intensity while unsubstituted **34** showed significant bathochromic shift of absorption maxima as well as the hypochromic effect of the intensity, similar to **24** and **32**. On the other hand, in water, **30** substituted with the isobutyl side chain showed the hypsochromic shift of absorption maxima while unsubstituted **34** showed significant bathochromic shift of absoprtion maxima as well as the hypechromic effect of the intensity. Compounds **24** and **32** also showed bathochromic shift of absorption maxima in comparison to compound **30** with hypochromic effect of absorption intensity.

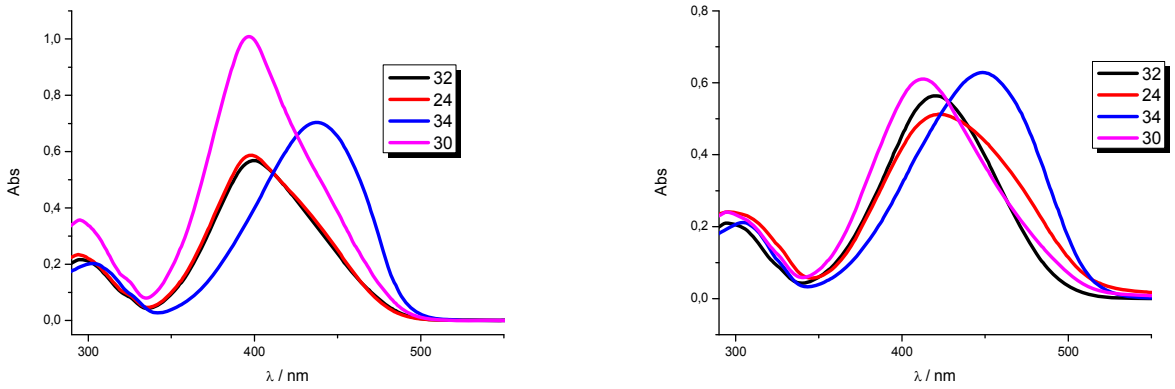

Figure 5. Absorption spectra of of **24**, **30**, **32** and **34** in dioxane (left) and water (right).

4. CONCLUSIONS

This manuscript presents the design and synthesis of novel unsubstituted and *N*-substituted imidazo[4,5-*b*]pyridine derived acrylonitriles prepared as potential antioxidants. The targeted compounds were substituted with variable number of methoxy groups or *N,N*-dimethyl(diethyl)amino group placed at the phenyl ring bearing either H atom, methyl, isobutyl and phenyl side chain at the N atom of imidazo[4,5-*b*]pyridine nuclei. Their antioxidative potential was studied with DPPH and ABTS spectroscopic assays, FRAP method and the electrochemical oxidation potential measurements.

Examined systems showed promising antioxidative potential through the FRAP assay, while in radical scavenging assays only three compounds displayed some activity. As the most active compound we identified the *N,N*-dimethylamino substituted **29** with the *N*-isobutyl moiety at the imidazo[4,5-*b*]pyridine core (Figure 6) showing the most pronounced FRAP activity of 2485.5 ± 4.2. Interestingly, all systems with the *N,N*-diethylamino group at the phenyl ring **24**, **30**, **32** and **34** also showed a significantly improved activity relative to a reference BHT. A reasonably good linear correlation found between FRAP activities and electrooxidation potentials implies that the scavenging effects of the studied compounds are related to their electrochemical behavior.

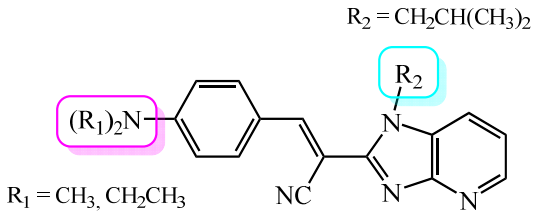

Figure 6. Structure of the most active system proposed as a lead compound.

Computational analysis confirmed the usefulness of the employed imidazo[4,5-*b*]pyridine derived acrylonitrile skeleton for the design of potent antioxidants and showed this activity predominantly resides in their ability to most efficiently transfer the hydrogen atom from the N–H and C–H bonds. It also revealed that investigated antioxidative capacity is efficiently improved either upon the *N*-alkylation of the imidazole nitrogen or through introducing strong electron-donating *para*-substituents on the distant phenyl unit, where *N*,*N*-dialkylamines prevail over methoxy groups. As a future perspective, DFT calculations also demonstrated that the attached cyano group works towards lowering the antioxidative potential of the examined systems and attempts to prepare similar derivatives without it are along the way.

Additionally, the spectroscopic properties of chosen compounds were studied in several polar and non-polar solvents. Obtained absorption spectra revealed that we can observed the strong impact of the substituent placed at the N atom of imidazo[4,5-*b*]pyridine nuclei as well as the polarity of solvents on the spectroscopic characteristics.

Supplementary Materials: Figure S1–S52: NMR spectra of novel compounds. Figure S53: UV absorption spectra of studied compounds.

Author Contributions: Ida Boček: Conceptualization, Formal analysis, Investigation, Writing - Original Draft. **Kristina Starčević:** Formal analysis, Investigation, Writing - Original Draft. **Ivana Novak Jovanović:** Formal analysis, Investigation, Writing - Original Draft. **Robert Vianello:** Formal analysis, Investigation, Writing - Original Draft. **Marijana Hranjec:** Conceptualization, Formal analysis, Investigation, Writing - Original Draft, Supervision.

Funding: This work was supported by the Croatian Science Foundation under the project 4379 entitled *Exploring the antioxidative potential of benzazole scaffold in the design of novel antitumor agents*, and the project 3163 entitled *Dietary lipids, sex and age in pathogenesis of metabolic syndrome*.

Declaration of Interest: The authors declare no conflict of interest.

5. REFERENCES

1. Joule, J.; Mills, K. Heterocyclic chemistry, 5th Edition, Blackwell Publishing Ltd, 2010.

2. Akhtar, W.; Faraz Khan, M.; Verma, G.; Shaquiquzzaman, M.; Rizvi, M.A.; Mehdi, S.H.; Akhter, M.; Mumtaz Alam, M. Therapeutic evolution of benzimidazole derivatives in the last quinquennial period. *Eur. J. Med. Chem.* 2017, 126, 705–753.
3. Rescifina, A.; Zagni, C.; Varrica, M.G.; Pistarà, V.; Corsaro, A. Recent advances in small organic molecules as DNA intercalating agents: Synthesis, activity, and modeling. *Eur. J. Med. Chem.* 2014, 74, 95–115.
4. Krause, M.; Foks, H.; Gobis, K. Pharmacological Potential and Synthetic Approaches of Imidazo[4,5-b]pyridine and Imidazo[4,5-*c*]pyridine Derivatives. *Molecules* 2017, 22, 399-424.
5. Taha, M.; Ismail, N.H.; Imran, S.; Rashwan, H.; Jamil, W.; Ali, S.; Kashif, S.M.; Rahim, F.; Salar, U.; Khan, K.M. Synthesis of 6-chloro-2-Aryl-1*H*-imidazo[4,5-*b*]pyridine derivatives: Antidiabetic, antioxidant, β-glucuronidase inhibiton and their molecular docking studies. *Bioorg. Chem.* 2016, 65, 48-56.
6. Cindrić, M.; Sović, I.; Martin-Kleiner, I.; Kralj, M.; Mašek, T.; Hranjec, M.; Starčević, K. Synthesis, antioxidative and antiproliferative activity of methoxy amidino substituted benzamides and benzimidazoles. *Med. Chem. Res.* 2017, 26, 2024–2037.
7. Tireli, M.; Starčević, K.; Martinović, T.; Kraljević Pavelić, S.; Karminski-Zamola, G.; Hranjec, M. Antioxidative and antiproliferative activities of novel pyrido[1,2-*a*]benzimidazoles. *Mol. Divers.* 2017, 21, 201–210.
8. Perin, N.; Roškarić, P.; Sović, I.; Boček, I.; Starčević, K.; Hranjec, M.; Vianello, R. Amino-Substituted Benzamide Derivatives as Promising Antioxidant Agents: A Combined Experimental and Computational Study. *Chem.Res. Toxicol.* 2018, 31, 974–984.
9. Neha, K.; Haider, M.R.; Pathak, A.; Shahar Yar, M. Medicinal prospects of antioxidants: A review. *Eur. J. Med. Chem.* 2019, 178, 687-704.
10. Tailor, N.; Sharma, M. Antioxidant hybrid compounds: a promising therapeutic intervention in oxidative stress induced diseases. *Mini Rev. Med. Chem.* 2013, 13, 280–297.
11. Lu, J. M.; Lin, P. H.; Yao, Q.; Chen, C. Chemical and molecular mechanisms of antioxidants: experimental approaches and model systems. *J. Cell. Mol. Med.* 2010, 14, 840–860.
12. Hybertson, B. M.; Gao, B.; Bose, S. K.; McCord, J. M. Oxidative stress in health and disease: the therapeutic potential of Nrf2 activation. *Mol. Aspects Med.* 2011, 32, 234–246.
13. Firuzi, O.; Miri, R.; Tavakkoli, M.; Saso, L. Antioxidant therapy: current status and future prospects. *Curr. Med. Chem.* 2011, 18, 3871-3888.
14. Kim, G.H.; Kim, J.E.; Rhie, S.J.; Yoon, S. The role of oxidative stress in neurodegenerative diseases. *Exp. Neurobiol.* 2015, 24, 325-340.
15. Foti, M.C. Use and abuse of the DPPH radical. *J. Agric. Food Chem.* 2015, 62, 8765–8776.
16. Ameta, R.K.; Singh, M. A thermodynamic in vitro antioxidant study of vitamins B (niacin and niacin amide) and C (ascorbic acid) with DPPH through UV spectrophotometric and physicochemical methods. *J. Mol. Liq.* 2014, 195, 40-46.

17. Cindrić, M.; Sović, I.; Mioč, M., Hok, L.; Boček, I.; Roškarić, P., Butković, K.; Martin-Kleiner, I.; Starčević, K., Vianello, R., Kralj, M., Hranjec, M. Experimental and Computational Study of the Antioxidative Potential of Novel Nitro and Amino Substituted Benzimidazole/Benzothiazole-2-Carboxamides with Antiproliferative Activity. *Antioxidants* 2019, 8, 477-499.
18. Perin, N.; Roškarić, P.; Sović, I.; Boček, I.; Starčević, K.; Hranjec, M.; Vianello, R. Amino-Substituted Benzamide Derivatives as Promising Antioxidant Agents: A Combined Experimental and Computational Study. *Chem. Res. Toxicol.* 2018, 31, 974–984.
19. Serdaroğlu, G.; Uludağ, N.; Ercag, E.; ugumar, P.; Rajkumar, P. Carbazole derivatives: Synthesis, spectroscopic characterization, antioxidant activity, molecular docking study, and the quantum chemical calculations. *J. Mol. Liq.* 2021, 330, 115651.
20. Altalhi, A.A.; Hashem, H.E.; Negm, N.A.; Mohamed, E.A.; Azmy, E.M. Synthesis, characterization, computational study, and screening of novel 1-phenyl-4-(2-phenylacetyl)-thiosemicarbazide derivatives for their antioxidant and antimicrobial activities. *J. Mol. Liq.* 2021, 333, 115977.
21. L. Hok, R. Vianello, Direct Metal-Free Transformation of Alkynes to Nitriles: Computational Evidence for the Precise Reaction Mechanism. *Int. J. Mol. Sci.* 2021, 22, 3193-4009.
22. Ptiček, L.; Hok, L.; Grbčić, P.; Topić, F.; Cetina, M.; Rissanen, K.; Kraljević Pavelić, S.; Vianello, R.; Racané, L. Amidino substituted 2-aminophenols: biologically important building blocks for the amidino- functionalization of 2-substituted benzoxazoles. *Org. Biomol. Chem.* 2021, 19, 2784–2793.
23. Tandarić, T.; Hok, L.; Vianello, R. From Hydrogen Peroxide-Responsive Boronated Nucleosides Towards Antisense Therapeutics – A Computational Mechanistic Study. *Croat. Chem. Acta* 2019, 92, 287–295.
24. Tandarić, T.; Vianello, R. Computational insight into the mechanism of the irreversible inhibition of monoamine oxidase enzymes by the anti-parkinsonian propargylamine inhibitors rasagiline and selegiline. *ACS Chem. Neurosci.* 2019, 10, 3532–3542.
25. Gaussian 16, Revision A.03, Frisch, M.J.; Trucks, G.W.; Schlegel, H.B.; Scuseria, G.E.; Robb, M.A.; Cheeseman, J.R.; Scalmani, G.; Barone, V.; Mennucci, B.; Petersson, G.A.; Nakatsuji, H.; Caricato, M.; Li, X.; Hratchian, H.P.; Izmaylov, A.F.; Bloino, J.; Zheng, G.J.; Sonnenberg, L.; Hada, M.; Ehara, M.; Toyota, K.; Fukuda, R.; Hasegawa, J.; Ishida, M.; Nakajima, T.; Honda, Y.; Kitao, O.; Nakai, H.; Vreven, T.; Montgomery Jr. J.A.; Peralta, J. E.; Ogliaro, F.; Bearpark, M.; Heyd, J.J.; Brothers, E.; Kudin, K.N.; Staroverov, V.N.; Kobayashi, R.; Normand, J.; Raghavachari, K.; Rendell, A.; Burant, J.C.; Iyengar, S.S.; Tomasi, J.; Cossi, M.; Rega, N.; Millam, J.M.; Klene, M.; Knox, J.E.; Cross, J.B.; Bakken, V.; Adamo, C.; Jaramillo, J.; Gomperts, R.; Stratmann, R.E.; Yazyev, O.; Austin, A.J.; Cammi, R.; Pomelli, C.; Ochterski, J.W.; Martin, R.L.; Morokuma, K.; Zakrzewski, V.G.; Voth, G.A.; Salvador, P.; Dannenberg, J.J.; Dapprich, S.; Daniels, A.D.,; Farkas, Ö.; Foresman, J.B.; Ortiz, J.V.; Cioslowski, J.; Fox, D. J. 2009, Gaussian 09, Revision A.02, Gaussian Inc., Wallingford, CT.
26. Huang, D.; Ou, B.; Prior, R.L. The Chemistry behind Antioxidant Capacity Assays. *J. Agric. Food Chem.* 2005, 53, 1841–1856.

27. Hu, C.; You, G.; Liu, J.; Du, S.; Zhao, X.; Wu, S. Study on the mechanisms of the lubricating oil antioxidants: Experimental and molecular simulation. *J. Mol. Liq.* 2021, 324, 115099.
28. Benayahoum, A.; Bouakkaz, S.; Bordjiba, T.; Abdaoui, M. Antioxidant activity and pK_a calculations of 4‐mercaptostilbene and some derivatives: A theoretical approach. *J. Mol. Liq.* 2019, 275, 221-231.
29. Marković, Z.; Tošović, J.; Milenković, D.; Marković, S. Antioxidants vs. Oxidative Stress: Insights from Computation. *Comput. Theor. Chem.* 2016, 1077, 11–17.
30. Daga, M.C.; Taddeia, M.; Varchib, G. Rapid microwave-assisted deprotection of N-Cbz and N-Bn derivatives. *Tetrahedron Lett.* 2001, 42, 5191-5194.
31. Kamila, S.; Ankati, H.; Mendoza, K.; Biehl, E.R. Synthesis of Novel Pyridobenzimidazoles Bonded to Indoleorbenzo[*b*]thiophenestructures. *Open Org. Chem. J.* 2011, 5, 127-134.
32. L. Bukowski, R. Kaliszan, Imidazo[4,5-*b*]pyridine derivatives of potential tuberculostatic activity. *Archiv der Pharmazie* 1991, 324, 121-127.
33. Darweesh, A.F.; Abd El-Fatah, N.A.; Abdel-Latif, S.A.; Abdelhamid, I.A.; Elwahy, A.H.M.; Salem, M.E. Synthesis and DTF studies of novel aminoimidazodipyridines using 2-(3*H*-imidazo[4,5-*b*]pyridin-2-yl)acetonitrile as an efficient key precursor. *ARKIVOC* 2021, vii, 23-37.
34. Perin, N.; Hok, L.; Beč, A.; Persoons, L.; Vanstreels, E.; Daelemans, D.; Vianello, R.; Hranjec, M. N-substituted benzimidazole acrylonitriles as in vitro tubulin polymerization inhibitors: synthesis, biological activity and computational analysis. *Eur. J. Med. Chem.* 2021, 211, 113003.
35. van Acker, S.A.B.E.; van den Berg, D.J.; Tromp, M.N.J.L.; Griffionen, D.H.; van Bennekom, W.P.; van der Vijgh, W.J.F.; Bast, A. Structural aspects of antioxidantactivity of flavonoids. *Free Radical Biol. Med.* 1996, 20, 331-342.
36. Yang, B.; Kotani, A.; Aria, K.; Kusu, F. Estimation of antioxidant activities of flavonoids from their oxidation potentials. *Anal. Sci.* 2001, 17, 599–604.
37. Komorsky-Lovrić, Š.; Novak Jovanović, I. Abrasive stripping square wave voltammetry of some natural antioxidants. *Int. J. Electrochem. Sci.* 2016, 11, 836–842.
38. Hotta, H.; Nagano, S.; Ueda, M.; Tsujino, Y.; Koyama, J.; Osakai, T. Higher radical scavenging activities of polyphenolic antioxidants can be ascribed to chemical reactions following their oxidation. *Biochim. Biophys. Acta* 2002, 1572, 123–132.
39. Firuzi, O.; Lacanna, A.; Petrucci, R.; Morrosu, G.; Saso, L. Evaluation of the antioxidant activity of flavonoids by "ferric reducing antioxidant power" assay and cyclic voltammetry. *Biochim. Biophys. Acta* 2005, 1721, 174–184.
40. Aertega, J.F.; Ruiz-Montoya, M.; Palma, A.; Alonso-Garrido, G.; Pintado, S.; Rodríguez-Mellado, J.M. Comparison of the simple cyclic voltammetry (CV) and DPPH assays for the determination of antioxidant capacity of active principles, *Molecules* 2012, 12, 5126–5138.

41. Abreu, R.; Falcão, S.; Calhelha, R.C.; Ferreira, I.C.F.R.; Queiroz, M.J.R.P.; Vilas-Boas, M. Insights in the antioxidant activity of diarylamines from the 2,3-dimethylbenzo[*b*]thiophene through the redox profile. *J. Electroanal. Chem.* 2009, 628, 43-47
42. Estevão M.S.; Luísa C. Carvalho L.C.; Ferreira L.M.; Fernandes E.; Marques M.M.B. Analysis of the antioxidant activity of an indole library: cyclic voltammetry versus ROS scavenging activity. *Tetrahedron Lett.* 2011, 52, 101-106.
43. Lucarini, M., Pedrielli, P.; Pedulli, G.F.; Valgimigli, L.; Gigmes, D., Tordo, P. Bond Dissociation Energies of the N−H Bond and Rate Constants for the Reaction with Alkyl, Alkoxyl, and Peroxyl Radicals of Phenothiazines and Related Compounds. *J. Am. Chem. Soc.* 1999, 121, 11546-11553.
44. Wang, L.; Yang, Q.; Li, Y.; Wang, S.; Yang, F.; Zhao, X. How the functional group substitution and solvent effects affect the antioxidant activity of (+)-catechin? *J. Mol. Liq.* 2021, 327, 114818.
45. Yüksek, H.; Koca, E.; Gürsoy-Kol, Ö.; Akyıldırım, O.; Çelebier, M. Synthesis, in vitro antioxidant activity, and physicochemical properties of novel 4,5-dihydro-1*H*-1,2,4-triazol-5-one derivatives. *J. Mol. Liq.* 2015, 206, 359-366.